Published in final edited form as:
Sci Signal. ; 3(107): ra8. doi:10.1126/scisignal.2000568.

Noncoding RNA Gas5 Is a Growth Arrest and Starvation-Associated Repressor of the Glucocorticoid Receptor

Tomoshige Kino[1,*], **Darrell E. Hurt**[2], **Takamasa Ichijo**[1], **Nancy Nader**[1], and **George P. Chrousos**[3]

[1]: Unit on Molecular Hormone Action, Program in Reproductive and Adult Endocrinology, *Eunice Kennedy Shriver* National Institute of Child Health and Human Development, National Institutes of Health, Bethesda, MD 20892, USA

[2]: Bioinformatics and Scientific IT Program, Office of Technology Information Systems, National Institute of Allergy and Infectious Diseases, National Institutes of Health, Bethesda, MD 20892, USA

[3]: First Department of Pediatrics, Athens University Medical School, Athens 11527, Greece

Abstract

The availability of nutrients influences cellular growth and survival by affecting gene transcription. Glucocorticoids also influence gene transcription and have diverse activities on cell growth, energy expenditure, and survival. We found that the growth arrest-specific 5 (Gas5) noncoding RNA, which is abundant in cells whose growth has been arrested due to lack of nutrients or growth factors, sensitized cells to apoptosis by suppressing glucocorticoid-mediated induction of several responsive genes, including the one encoding cellular inhibitor of apoptosis 2. Gas5 bound to the DNA-binding domain of the glucocorticoid receptor (GR) by acting as a decoy “glucocorticoid response element (GRE)”, thus, competing with DNA GREs for binding to the GR. We conclude that Gas5 is a ribo-repressor of the GR, influencing cell survival and metabolic activities during starvation by modulating the transcriptional activity of the GR.

Introduction

The environment, together with the intrinsic state of the organism, direct constituent cells to rest, grow, proliferate, differentiate, or undergo apoptosis. One of the key regulators dictating

*: Corresponding author. Address correspondence and requests for materials and reprints to: Tomoshige Kino, M.D., Ph.D., Unit on Molecular Hormone Action, Program in Reproductive and Adult Endocrinology, *Eunice Kennedy Shriver*, National Institute of Child Health and Human Development, National Institutes of Health, Bldg. 10, Clinical Research Center, Rm. 1-3140, 10 Center Drive MSC 1109, Bethesda, MD 20892-1109, USA, Phone: 301-496-6417, Fax: 301-402-0884, kinot@mail.nih.gov.

Overline: Molecular Biology

One sentence summary: Gas5 is a noncoding RNA that acts as a decoy glucocorticoid response element to inhibit glucocorticoid-mediated transcription.

Editor's Summary:

Noncoding RNA Decoys

Steroid receptors are transcription factors that are activated by ligand binding, which allows these proteins to bind specific sequences called "response elements" in the promoters of target genes to stimulate transcription. Now, Kino et al. find that a noncoding RNA can also interact with steroid receptors and inhibit their binding to the DNA response elements, thereby repressing steroid receptor activity. The authors found that the noncoding RNA growth arrest-specific 5 (Gas5), which accumulates in cells that have been deprived of nutrients or growth factors, bound to the glucocorticoid receptor and competed with DNA glucocorticoid response elements for binding to the receptor, thereby inhibiting glucocorticoid-mediated transcription. This sensitized cells to undergo apoptosis in response to stress by preventing the glucocorticoid-mediated transcription of antiapoptotic genes. Gas5 also interacted with other steroid receptors and inhibited their transcriptional activity, suggesting that decoy RNA "response elements" may be a common mechanism for regulating transcription factor activity.

cellular behavior is the availability of nutrients, which controls cell growth. Nutrient status modulates the abundance, activity, or both of numerous transcription factors, which alters the transcriptional profiles of certain sets of genes, including those encoding proteins involved in energy metabolism and stress responses at the cellular level, and those encoding proteins involved in the immune response at the organismal level (1,2).

Steroid hormones are intercellular mediators, linking alterations in the environment or the body's intrinsic states, or both, to cellular activities. One class of such hormones, the glucocorticoids, play diverse physiological roles in the regulation of basal-and stress-related homeostasis in all extant gnathostomes (3,4). These hormones generally shift the body's metabolic activities toward catabolism, modulate immune function, and influence cell survival by altering the cell's sensitivity to apoptosis in response to external or internal stress (4–7). Pharmacologically, glucocorticoids are powerful immunosuppressive and antineoplastic agents important to human therapeutics (4). Because glucocorticoids have potent and diverse influences on numerous functions, not only is glucocorticoid production strictly regulated, but so is tissue responsiveness (5,8). Indeed, glucocorticoid action in cells is specifically adjusted during different phases of the cell cycle (9,10), and several autoimmune, allergic, and inflammatory disorders, metabolic syndromes, and infection with the human immunodeficiency virus type-1 have been associated with alterations in the responsiveness of specific organs and tissues to glucocorticoids (5,8,11). Underlying mechanisms(s) for the alterations of local glucocorticoid actions, however, have not been well elucidated as yet.

Most of the known biological actions of glucocorticoids are mediated by the glucocorticoid receptor (GR), one of the nuclear receptor superfamily proteins and a hormone-dependent transcription factor (3,5). After binding with a glucocorticoid agonist, the GR translocates from the cytoplasm into the nucleus and binds, through its DNA-binding domain (DBD), to glucocorticoid response elements (GREs) in the regulatory regions of glucocorticoid-responsive genes (5,12). Promoter-bound and activated GR then attracts coactivators and chromatin-remodeling factors, as well as RNA polymerase II and its ancillary factors, to stimulate the transcription of responsive genes (5). Alternatively, glucocorticoid agonist-bound GR may interact with other transcription factors, altering their transcriptional effects on their specific responsive genes (3,5).

Expanding numbers of noncoding RNAs (ncRNAs) with regulatory functions have been reported (13). These molecules are present throughout evolution from viruses and bacteria to plants and higher eukaryotic animal cells. NcRNAs affect every aspect of organismal biology by influencing the abundance of proteins by affecting mRNA transcription, degradation, and translation, or by influencing the nuclear translocation of proteins, or by influencing both protein abundance and localization (13,14). One such single-strand ncRNA, the growth arrest-specific 5 (Gas5), was so named because it accumulated in growth-arrested cells (15). Its encoding gene, *gas5*, is one of the 5′-terminal oligopyrimidine (5′TOP) class genes, characterized by an upstream oligopyrimidine tract sequence (16,17). Growth arrest by serum starvation or treatment with inhibitors of protein translation is associated with attenuated translation of 5′TOP RNAs and the inhibition of their degradation (18), resulting in marked accumulation of spliced, mature Gas5 RNA (17). The functions of Gas5 ncRNA are not well known as yet; however, the *gas5* gene, in addition to Gas5 ncRNA, expresses from its intronic sequences multiple small noncoding nucleolar RNAs (snoRNAs) that are involved in the biosynthesis of ribosomal RNA (17) (Fig. 1).

We found that Gas5 ncRNA interacted with the DBD of the ligand-activated GR through a decoy RNA "GRE" and suppressed GR-induced transcriptional activity of endogenous glucocorticoid-responsive genes by inhibiting binding of GRs to target genes' GREs. Our

results indicate that Gas5 ncRNA functions as a starvation-linked or growth arrest-linked riborepressor of the GR and possibly other steroid hormone receptors.

Results

To identify factors that regulate the transcriptional activity of the GR, we performed a LexA-based yeast two-hybrid screen with the human Jurkat cell cDNA library, using the GR DBD as bait. Out of 118 clones, we found 2 independent clones that contained the Gas5 sequence starting around 55 bps downstream of its transcription initiation site. We speculated that the Gas5 RNA directly interacted with the bait GR DBD. Because ncRNAs interact with proteins, which are important for the maintenance of ncRNAs' 3-dimensional structure and biological functions (19,20), we speculate that Gas5 may have evoked a positive signal in the yeast two-hybrid screen through such putative Gas5-associated proteins, possibly free histones, transcriptional cofactors or similar molecules (5,21).

The *gas5* gene does not express proteins from its exons (17); however, it does encode several ncRNAs both in exonic and intronic sequences (Fig. 1). Thus, we examined the potential interaction of Gas5 ncRNA and GR with an RNA and protein coimmunoprecipitation assay in HeLa cells, which endogenously express these molecules (Fig. 2A). Dexamethasone, a GR agonist, increased the association of GR with Gas5 RNA as shown by coprecipitation with an antibody that recognizes the LBD of the GR (anti-GR Ab). Association of Gas5 to GR was observed with concentrations of dexamethasone as low as 10^{-10} M, which is more than 10-times lower than the concentration equivalent to physiologic free levels of circulating cortisol (4). In contrast, GR did not interact with negative control RNAs miR191 and SC53 (Fig. 2B), nor did GR interact with another negative control U75 snoRNA (Fig. 2C), which is expressed from the *Gas5* intronic sequence. We detected an interaction between GR and the transfer RNA (*t*RNA) for arginine [*t*RNA(Arg)], which was previously reported to bind GR and thus served as a positive control (22) (Fig. 2C). Further, Gas5 ncRNA associated with GR in a DBD-dependent fashion, because the GR chimera, G-gal-G, in which the DBD was replaced with that of the bacterial transcription factor GAL4, had no such interaction (Fig. 1D). In a reporter assay in which Gas5 ncRNA and GR were overexpressed and glucocorticoid-responsive mouse mammary tumor virus (MMTV) promoter was employed as a reporter, Gas5 significantly suppressed dexamethasone-stimulated transcriptional activity of the wild type GR in GR-deficient HCT116 cells, whereas it did not affect that of G-gal-G (Fig. 2E). We ruled out the possibility that Gas5 acts on GR through a translated protein by showing that it was effective in the reporter assay in the presence of the translation inhibitor cycloheximide (fig. S1). Thus, Gas5, as RNA, is associated with the DBD of GR in the presence of ligand and suppresses GR-induced transcriptional activity in a DBD-dependent fashion.

We examined the subcellular localization of Gas5 in HeLa cells with RNA fluorescent in situ hybridization. Gas5 was localized both in the cytoplasm and the nucleus, but its presence was more prominent in the former compartment in agreement with a previous report (16) (Fig. 3A, top panels). In the presence of dexamethasone, a fraction of Gas5 translocated into the nucleus, whereas a GR binding-defective Gas5 mutant (GRE-1 Mut) failed to translocate into the nucleus (Fig. 3B). A nuclear localization signal 1 (NL1)-defective GR mutant with diminished nuclear translocation activity upon binding to glucocorticoids (23) reduced Gas5 nuclear translocation in HCT116 cells (Fig. 3C). We also calculated the number of Gas5 RNA molecules in the presence and absence of dexamethasone in HeLa cells (table S1) and found that dexamethasone increased Gas5 copy numbers in the nucleus, consistent with the results shown in fig. 2. These results collectively indicate that Gas5 interacts with ligand-activated GR through its DBD in the cytoplasm and comigrates with GR into the nucleus.

Glucocorticoids impact cell survival decisions, by causing apoptosis by themselves or by changing the vulnerability of cells to apoptotic stimuli (6,7,24). For example, glucocorticoids induce apoptosis in lymphoid cells (6), whereas they inhibit apoptosis in several epithelial cells, including HCT116 and HeLa cells, by stimulating the expression of the gene encoding cellular inhibitor of apoptosis 2 (cIAP2) (7,24,25). This protein binds cell death proteases caspase 3, 7, and 9 and inhibits their activities, thereby suppressing apoptosis triggered by treatment with Fas-ligand or tumor necrosis factor α (TNF-α) (7,26). The *cIAP2* gene promoter has imperfect tandem GREs ~500 base pairs (bps) upstream of its transcriptional initiation site and GR activates its transcription by binding to these GREs (24,25). Thus, we examined the effect of overexpressed Gas5 on the binding of GR to the *cIAP2* GREs. We transfected increasing amounts of a Gas5-expressing plasmid into HeLa cells, and performed chromatin immunoprecipitation (ChIP) assays with a primer pair specific for the *cIAP2* GREs and a GR antibody that recognizes the LBD of the GR (Fig. 4). In the same experiments, we purified total RNA from aliquots of suspended cells and monitored the abundance of the *cIAP2* mRNA and Gas5 ncRNA by real-time PCR (Fig. 4B and C). Gas5 suppressed both binding of GR to *cIAP2* GREs and *cIAP2* mRNA expression in a dose-dependent fashion (Fig. 4A, B), indicating that Gas5 inhibited association of GR with the *cIAP2* GREs and repressed GR-induced transcriptional activity of the *cIAP2* gene. To rule out the possibility that anti-GR antibody employed in the ChIP assays interfered with the binding of GR to *cIAP2* GREs, we performed the ChIP assay with another antibody that recognizes the GR N-terminal domain (NTD), in addition to the antibody that recognized the LBD of GR, and Gas5 suppressed association of GR to *cIAP2* GREs regardless of the antibody employed (Fig. 4, fig. S2).

We also tested the effects of Gas5 ncRNA on other well-known glucocorticoid-responsive genes in HeLa and HepG2 cells. These were the genes encoding the glucocorticoid-induced leucine zipper protein (GILZ), the serum/glucocorticoid-regulated kinase 1 (SGK1), the phosphoenolpyruvate carboxykinase (PEPCK), and the glucose 6 phosphatase (G6Pase) genes, all of which contain functional GREs in their promoter regions (27–30) (Fig. 5). Overexpressed Gas5 suppressed dexamethasone-induced mRNA expression of all these genes (Fig. 5A), as well as the association of the GR to their GREs (Fig. 5B). In contrast, Gas5 did not influence the transcriptional activity of the peroxisome proliferators-activated receptor δ (PPARδ) on its target gene encoding adipose differentiation-related protein (ADRP) and did not affect the binding of PPARδ to PPAR response elements located in the promoter region of the *ADRP* gene (31) (Fig. 5A, B). We confirmed that Gas5 did not alter the abundance of either GR or PPARδ by Western blotting (Fig. 5C).

To examine the effect of endogenous Gas5 on the transcription of the *cIAP2* and the *SGK1* genes, we cultured HeLa cells in serum-free medium for up to 96 hours to promote the accumulation of endogenous Gas5 (Fig. 6). We compared cells transfected with control siRNA or siRNA that specifically knocked down Gas5, but not snoRNAs produced by the *gas5* gene. Thymidine incorporation into the cells gradually decreased during the time of incubation, indicating that a progressively increasing number of these cells stopped growing (Fig. 6A). Gas5 ncRNA increased up to 7-fold (when comparing cells cultured in the presence of serum and the absence for 96 hours) in control siRNA-transfected cells, and it was strongly suppressed in Gas5 siRNA-transfected cells (Fig. 5B). Dexamethasone-induced *cIAP2* and *SGK1* transcription was also attenuated in the presence of control siRNA, and it was restored in the presence of Gas5 siRNA (Fig. 6C, D). These results indicate that endogenous Gas5 ncRNA accumulates in cells growth-arrested in response to serum withdrawal and acts as a negative regulator of GR-induced transcription of the endogenous glucocorticoid-responsive *cIAP2* and *SGK1* genes.

Because the *gas5* gene encodes multiple snoRNAs in addition to Gas5 ncRNA (17) (Fig. 1), we examined the expression of one such snoRNA, U75, in HeLa cells transfected with Gas5

siRNA and incubated in serum-free medium (fig. S3). Gas5 ncRNA increased in cells incubated with serum-free medium, and Gas5 siRNA suppressed this change (fig. S3B). U75 snoRNA weakly increased in response to serum withdrawal, and the Gas5 siRNA did not affect the abundance of this RNA (fig. S3C). Dexamethasone-induced *cIAP2* mRNA expression correlated negatively with Gas5 ncRNA, but did not correlate with the abundance of U75 snoRNA (fig. S3A). These results suggest that snoRNAs expressed from the *gas5* gene do not contribute to the suppressive effect of Gas5 on dexamethasone-induced *cIAP2* mRNA expression.

cIAP2 and SGK1 are apoptosis inhibitors (26,32). To further address physiologic implications of Gas5 on glucocorticoid-mediated induction of the *cIAP2* and the *SGK1* genes, we cultured HeLa cells transfected with Gas5 siRNA or control siRNA in serum-free medium for 72 hours and treated them with a Fas antibody and interferon (IFN) γ for an additional 24 hours to induce apoptosis (Fig. 7A). The Fas antibody and IFN-γ treatment induced apoptosis in about 25% of the cells transfected with control siRNA, and dexamethasone significantly prevented apoptosis, which is consistent with previous reports (Fig. 7A) (7,24). Gas5 siRNA did not influence induction of apoptosis in the absence of dexamethasone, however, it increased cell survival in response to dexamethasone treatment (Fig. 7A). Caspase 3, 7 and 9 whose activities are suppressed in response to the anti-apoptotic cIAP2 and SGK1 (7,26,33) were consistently altered parallel to the apoptotic changes (Fig. 7B, C). Taken together, these results suggest that Gas5 accumulated in cells growth-arrested in response to serum withdrawal and suppressed the dexamethasone-induced anti-apoptotic effect, which made the cells more sensitive to apoptotic stimuli. The repression of GR-induced transcriptional activity of the glucocorticoid-responsive antiapoptotic genes, such as *cIAP2* and the *SGK1*, likely contributed to the proapoptotic activity of Gas5.

To examine the molecular mechanism(s) by which Gas5 ncRNA repressed the transcriptional activity of GR, we identified the portion of Gas5 responsible for its binding to GR and hence potentially crucial for the transcriptional repression of this receptor (Fig. 8). Full-length Gas5 ncRNA and its fragments containing the 400–598 sequence bound GR in response to dexamethasone and suppressed GR-induced transcriptional activity, whereas Gas5 fragments devoid of this RNA portion were also devoid of these effects (Fig. 8A, B). We confirmed that the abundance of the Gas5 fragments and GR in cells expressing these fragments were similar (fig. S4 A, B). Thus, the region of the Gas5 sequence between nucleotides 400 and 598 is responsible for both binding to the GR and for inhibiting the transcriptional activity of this protein (Fig. 8C).

This portion of Gas5 contains 6 hairpin structures and hairpin #5, which we call the Gas5 “GRE-mimic”, contains two GRE-like sequences at nucleotides 539–544 (“GRE-1”) and 553–559 (“GRE-2”). These sequences are predicted by UNAFold (34) to double back and complement each other forming a hairpin structure, which is supported in part by the RNA-specific Wobble base-pairing (35) between uracil and guanine (Fig. 8D). The Gas5 GRE-mimic has G540 in the 5′ strand and C554 in the 3′ strand (shown with black boxes in Fig. 8D), which are conserved in the consensus DNA GREs, and play a critical role in specifying the affinity of the DNA GREs to the GR DBD through formation of hydrogen bonds with K442 and R447 of the latter (36). Although the mouse and human Gas5 exonic sequences share ~70% nucleotide homology (16,17), the GRE-mimic sequences in human Gas5 are conserved in mouse Gas5, which is the only other species in which the Gas5 sequence that has been reported to date. We also found a “mineralocorticoid response element” (MRE)-like sequence at nucleotides 473–478 of hairpin #3, which did not have a perfectly complementing sequence, but was still predicted to form a double helical structure.

To examine the specificity of the ncRNA GRE or MRE sequences, we created plasmids expressing various Gas5 mutants. Gas5 “GRE-1 Mut” and “GRE-2 Mut” have base substitutions in GRE-1 and GRE-2, respectively, which disrupts double helical structure of hairpin #5. In contrast, Gas5 “GRE-1/2 Mut Helix” has mutations that disrupt conserved nucleotides in “GRE-1” and “GRE-2” but still forms a double-stranded structure (for details, see fig. S5). In HCT116 cells, all of these mutant Gas5 ncRNAs failed to inhibit GR-induced transcription of the MMTV promoter (fig. 8E). In contrast, mutation of the “MRE” in Gas5 ncRNA preserved the repressive effect, suggesting that this sequence has no functional significance as far as GR activity is concerned. Furthermore, when expressed in HeLa cells, Gas5 GRE-1 Mut did not suppress dexamethasone-induced *cIAP2* mRNA expression and did not prevent the association of GR to *cIAP2* GREs; whereas wild type Gas5 blocked the GR interaction with the *cIAP2* GREs and dexamethasone induction of *cIAP2* mRNA (Fig. 8F).

We examined binding activity of Gas5 ncRNA to the GR DBD in an in vitro binding assay (Fig. 9A). Wild type Gas5 ncRNA bound glutathione-*S* transferase (GST)-fused to the GR DBD, whereas it did not bind GST. Addition of increasing amounts of double-stranded DNA GREs attenuated the association of Gas5 ncRNA to the GR DBD in a dose-dependent fashion, whereas addition of the mutated DNA GREs did not affect this association. Neither Gas5 GRE-1 Mut, GRE-2 Mut, nor GRE-1/2 Mut Helix RNAs bound to the GR DBD. Thus, the RNA GRE sequences of GRE-1 and GRE-2 and the double helical structure formed by these RNA GREs are both necessary for Gas5 to bind GR DBD. The dissociation constant (Kd) of Gas5 to GR DBD in this in vitro system was ~30 nM (Fig. 9B), whereas that of GRE DNA to GR DBD was reported to be ~60 nM (37).

With an in vitro binding assay, we found that Gas5 ncRNA competed with DNA GREs for binding to the GR DBD (Fig. 9C). Addition of increasing amounts of wild type Gas5 RNA suppressed the association of fluorescein (FAM)-labeled DNA GREs to the GR DBD in a dose-dependent fashion, whereas Gas5 GRE-1 Mut did not. Wild type Gas5 RNA demonstrated ~3 times stronger displacing activity than the DNA GREs, which is consistent with the affinity of Gas5 RNA for GR DBD that we found.

We used the secondary structure predictions from UNAFold (38) to guide tertiary structure predictions for the Gas5 RNA GRE-mimic and MRE-resembling region (Fig. 9D). Although several structure solutions were calculated, the GRE-mimic and MRE-resembling regions maintained their local base pairing among all the calculated configurations. This local base pairing was used as a constraint for tertiary structure prediction of these regions using Rosetta (39). The top 1000 decoys from each region were clustered. In both predictions, the lowest-energy decoy was part of the largest cluster and was chosen as the best representative solution (Fig. 9D, right three structures). Critical GR DBD residues K442 and R447 insert into the major groove and interact with base pairs (shown in red) of the DNA GRE on its opposite strands separated by a half turn (Fig. 9D, left structure) (19). The prediction for the structure of the Gas5 GRE-mimic placed the two base pairs (G540 and C554, shown in red) analogous to those of the DNA GRE on opposing strands separated by a half turn and pointing into the pseudo major groove, mimicking the DNA structure (Fig. 9D, middle 2 structures). In comparison, the prediction for the structure of the Gas5 MRE-resembling region placed the two analogous base pairs (U453 and G474, shown in red) on opposing strands separated by a full turn on the pseudo minor groove and pointing away from each other along the major axis of the pseudo helix (Fig. 9D, right structure). These models suggest a plausible structural explanation for the binding of Gas5 GRE-mimic to GR DBD and the lack of such binding of the Gas5 MRE-resembling region.

To verify these predictions, we created mutant GRs defective in K442 and R447 and performed in vitro and in vivo binding assays. Replacement of either K442 or R447 by alanine

significantly reduced the binding activity of the mutated GR DBDs to Gas5 ncRNA in an in vitro binding assay, and simultaneous replacement of these residues completely abolished binding (Fig. 9E). Further, the GR mutants harboring K442A or R447A, or both, lost their binding activity to Gas5 ncRNA in HCT116 cells (Fig. 9F). All of the GR mutants that we employed in the assay appeared to have stable protein structure, because they interacted with a GR antibody and their abundance was similar in HCT116 cells (Fig. 9F), while some of them were reported to have a stability similar to that of wild type GR in yeast (40). Taken together, these results indicate that Gas5 binds the GR DBD through its GRE-mimic region, imitating the binding of DNA GRE to the GR.

Because other steroid receptors, for example the mineralocorticoid (MR), progesterone (PR), and androgen (AR) receptors, share some of the same response sequences with the GR, we examined the effect of Gas5 on MR-, PR- and AR-induced transactivation of the MMTV promoter in HCT116 cells (Fig. 10). As expected, Gas5 suppressed the transcriptional activity of MR, PR-A, and AR, in addition to that of GR, in a ligand-dependent fashion. Gas5 did not influence the transcriptional activity of estrogen receptor α (ERα), PPARδ, p53, or the VP16 activation domain fused with the GAL4 DBD (Fig. 10B). Accordingly, Gas5 bound DBD of the MR, AR, and PR-A, but not that of ERα, in an in vitro binding assay (Fig. 10C). These results indicate that Gas5 may function as a general corepressor of some steroid hormone receptors, repressing transcriptional activity possibly by binding to their DBDs.

Discussion

Our results indicate that Gas5 ncRNA functions as a starvation or growth arrest-linked riborepressor for the GR, and possibly other steroid hormone receptors, by binding to their DBD through its double-stranded RNA GRE-mimic and, thereby, inhibiting the association of these receptors with their DNA recognition sequence. Gas5 is mechanistically related to the bacterial 6*S* RNA, which binds RNA polymerase and inhibits transcription by mimicking the open promoter, to which the RNA polymerase binds (14,41). Gas5 that accumulates in growth-arrested cells may alter cell fate by making the cells more or less susceptible to apoptotic and other growth-related stimuli through modulation of steroid hormone activities. Fasting appears to increase the abundance of Gas5 and Gas5 suppresses dexamethasone-stimulated transcription of genes encoding the enzyme glucose-6-phosphatase (G6Pase) and phosphoenolpyruvate carboxykinase (PEPCK), enzymes that play key roles in glucose metabolism, functioning as rate-limiting for gluconeogenesis and glycogenolysis, respectively (42). Thus, Gas5 may also help save energy resources as an adaptive response to starvation by restricting the expression of steroid-responsive genes, possibly in an organ- or tissue- and gene-specific fashion.

Gas5 was reported to act as a sensitizer of apoptosis (43). Our results showing that Gas5 makes cells more susceptible to apoptosis by inhibiting the anti-apoptotic action of glucocorticoids may be a mechanism for the proapoptotic actions of Gas5. The *gas5* gene is located in the disease susceptibility locus in mouse BXSB strain, which develops glomerulonephritis associated with systemic lupus erythematosus (44). Because glucocorticoids are potent immunosuppressants, frequently used in the treatment of autoimmune diseases, elevated expression of Gas5 might play a role in the development of such autoimmunity-based disorders by suppressing glucocorticoid action on immune or immune-accessory cells.

Over 2 decades ago, RNAs, such as transfer RNAs (*t*RNAs) and synthetic polyribonucleotides, were reported to bind steroid receptors, preventing these receptors from binding their target DNA sequences (22,45,46). Interestingly, RNA purified from White Leghorn chicks and MCF-7 cells inhibited the association of the vitamin D receptor, the estrogen receptor, and the GR with their respective DNA response sequences (45,47). These previous reports indicated

that some RNAs residing in animal tissues could influence functions of steroid receptors by inhibiting their interaction with DNA. In agreement with these previous reports, we demonstrate here that Gas5 binds the GR DBD and suppresses GR-induced transcriptional activity. Thus, particular groups of ncRNAs, including Gas5 and *t*RNA, may be an integral component of the regulatory machinery for adjusting steroid hormone activity in target tissues. Indeed, another ncRNA, steroid receptor RNA coactivator (SRA), enhances nuclear receptor-induced transcriptional activity as part of the initiation complex, whereas it represses the transcriptional activity of nuclear receptors by associating with SLIRP, a stem-loop interacting protein (48). Similarly, Pus1p, a pseudo-uridine synthase, modulates SRA activity through a physical interaction (48). As with SRA, association of partner proteins to ncRNAs are important for enabling the latter to exert their actions, thus it is quite intriguing to examine whether Gas5 has the ability to mimic the conformation of chromatin-integrated DNA interaction with histone-bound proteins or other chromatin components with which the GR normally interacts to stimulate transcription of endogenous, glucocorticoid-responsive genes (5).

Materials and Methods

Plasmids

pcDNA3-Gas5(1-598) was constructed by subcloning the full Gas5 sequence lacking a poly A tail (based on the Gas5 sequences reported as AF141346 and NR_002578 in GenBank), amplified from total RNA purified from HeLa cells into pcDNA3 (Invitrogen, Carlsbad, CA). pcDNA3-Gas5(55-598), (199-598), (400-598), (1-201), (55-201), (1-402) and (199-402) were constructed by subcloning the corresponding Gas5 cDNA fragments into pcDNA3. pcDNA3-Gas5(1-598) GRE-1 Mut, GRE-2 Mut, and GRE-1/2 Mut Helix, which express mutant Gas5 RNAs defective in hairpin #5 at nucleotides 539–544 and 553–559, respectively, were constructed by PCR-assisted mutagenesis reactions. pcDNA3-Gas5(1-598) MRE Mut expresses mutant Gas5 RNA defective in hairpin #3 at nucleotides 472–478. Gas5(1-598) GRE-1 Mut and GRE-2 Mut have nucleotide replacements destroying complementarity of hairpin #5, and thus, do not form the double-stranded structure. Gas5(1-598) GRE-1/2 Mut Helix has nucleotide replacements that destroy the original sequences of hairpin #5 but preserve the double-stranded structure (for more details, see fig. S5). pRShGRα and pRSG-gal-G were gifts from Dr. R. M. Evans (Salk Institute, La Jolla, CA). pGEX-4T3-GR DBD was described previously (49). pGEX-4T3-MR, -AR, -ERα and -PR-A DBD were created by subcloning the DBD of the human MR, AR, ERα, or PR-A into pGEX-4T3. pRShGRαK442A, R447A, and KR44/447AA, and pGEX-4T3-GR DBD K442A, R447A, and KR442/447AA, which respectively express GR or GST-fused GR DBD with corresponding mutations, were produced by PCR-assisted mutagenesis reactions. pRShGRαNL1^{-}, which expressed human GRα defective in NL1, was produced by introducing lysine (K) to asparagine (N) mutations at amino acids 494 to 496 of the human GRα by PCR-assisted mutagenesis reactions (23). pLexA-GR (420-489) was reported previously (50). pcDNAI/Amp-hMR, pSVLPRA, p5HB-hAR-A, HE0, pCMX-mPPARδ, pCMX-mRXRα, pCMV-p53, and pGAL4-VP16, which express the human MR, PR-A, AR, and ERα, and the mouse PPARδ, the retinoic X receptor (RXR) α, the human p53, and GAL4-fused VP16 activation domain (AD), respectively, were gifts from Drs. N. Warriar (Centre 71 Recherche Hôtel-Dieu Qué-bec and Laval Univ., Québec, Canada), S. S. Simons Jr. (National Institutes of Health, Bethesda MD), F. French (Univ. of North Carolina-Chapel Hill, Chapel Hill, NC), J.H. Segars (National Institutes of Health, Bethesda MD), R.M. Evans (Salk Institute, La Jolla, CA), B. Vogelstein (Johns Hopkins Univ., Baltimore MD) and Y. Shi (Harvard Medical School, Boston, MA), respectively. pMMTV-Luc, pERE-tk-Luc, pG13-Luc, and p17mer-tk-Luc, which respectively contain the glucocorticoid-responsive mouse mammary tumor virus (MMTV) promoter-, the synthetic vitellogenin A2 estrogen response elements-, the p53-responsive elements-, and the GAL4 response elements-driven

luciferase genes, are gifts from Drs. G.L. Hager (National Cancer Institute, Bethesda, MD), J.H. Segars, B. Vogelstein (Johns Hopkins Univ., Baltimore MD) and M-J. Tsai (Baylor College of Medicine, Huston, TX), respectively. pSV40-β-Gal and pGEX-4T3 were purchased from Promega (Madison, WI) and GE Healthcare Bioscience Corp. (Piscataway, NJ), respectively.

LexA-based yeast two-hybrid screening assay

Yeast two-hybrid screening assay was performed using the human GR(420-489) as bait in the human Jurkat cell cDNA library with the LexA system (Clontech Laboratories, Inc., Mountain View, CA).

Transfection and reporter assays

Human cervical carcinoma HeLa and human colon carcinoma HCT116 cells, which do and do not express functional GR, respectively, were used for reporter assays by transfecting them with Lipofectin™, as previously reported (51). These cells were transfected with Gas5-related plasmids together with pRShGRα or pRSG-gal-G, and pMMTV-Luc or p17mer-tk-Luc, in the presence of pSV40-β-Gal. Twenty-four hours after the transfection, cells were treated with 10^{-6} M of dexamethasone or vehicle and cell lysates were harvested after an additional 24 hours of incubation. Luciferase and β-galactosidase activities were measured, as previously reported (52). For blocking protein translation, 50 μM of cycloheximide were added to the medium of HeLa cells 2 hours before transfection and was kept throughout the experiment. HeLa cells and hepatocellular carcinoma HepG2 cells, which express endogenous GR and Gas5, were transfected with siRNAs or the Gas5-expressing plasmid by using the Nucleofector system (Amaxa GmbH, Cologne, Germany) (solution-R and protocol-I13 for HeLa cells, and solution-V and protocol-T28 for HepG2 cells) with over 70% transfection efficiency (51). siRNA for the human Gas5 (5′-CUUGCCUGGACCAGCUUAAdTdT-3′), which targets nucleotides 190–210 of the human Gas5 sequence (GenBank™ accession number NR_002578), and the negative control siRNA (5′-UUCUCCGAACGUGUCACGUdTdT-3′) were produced and purchased from Qiagen (Valencia, CA). Off-target effects of the Gas5 siRNA were verified using other siRNAs, which target Gas5 as well (fig. S6). HeLa cells were also transfected with FuGENE 6 (Roche Applied Bioscience, Indianapolis, IN) for RNA/protein coimmunoprecipitation assays.

SYBR Green real-time PCR

HeLa or HepG2 cells were transfected with Gas5 siRNA or plasmids and treated with compounds or medium indicated in respective experiments, and total RNA was purified with RNeasy or miRNeasy Mini Kit (Qiagen). The reverse transcription reaction was carried out with the TaqMan reverse transcription reagents (Applied Biosystems) (51), and the real-time PCR was performed in triplicate using the SYBR Green PCR Master Mix (Applied Biosystems), as previously described (53). The primer pairs used for examining mRNA or RNA abundance of ADRP, cIAP2, Gas5, G6Pase, GILZ, luciferase, PEPCK, RPLP0, SGK1, and U75 are shown in Table 1. Obtained C*t* (threshold cycle) values of ADRP, cIAP2, Gas5, G6Pase, GILZ, luciferase, PEPCK, SGK1, and U75 were normalized for those of RPLP0, and their relative mRNA expression was demonstrated as fold induction above the baseline, obtained in the absence of Gas5 expression and respective ligand. The dissociation curves of the used primer pairs showed a single peak, and after the PCRs, the samples had a single expected DNA band in agarose gel analysis.

Coimmunoprecipitation of GR and Gas5 RNA (RNA/protein co-precipitation assay)

Untransfected HeLa cells or cells transfected with Gas5 fragment-expressing plasmids were treated with 10^{-6} M of dexamethasone or vehicle for 5 hours, and the cells were subsequently

lysed in buffer containing 50 mM Tris-HCl [pH 7.4], 150 mM NaCl, 0.1% NP-40, 0.5% sodium deoxycholate and Complete™ protease inhibitor tablet (Roche Applied Bioscience) [1Tab/50ml] and 1 U/μl of the RNase inhibitor RNAsin (Promega). After spinning at 20,000*g* for 15 min, supernatant was used for precipitation of the GR/RNA complexes with GR antibodies or control rabbit IgG (Affinity Bioreagents, Golden, CO and Santa Cruz Biotechnologies, Inc., Santa Cruz, CA). Coprecipitated RNA was purified with TRIZOL™ reagent (Invitrogen), treated with DNase (Promega), reverse transcribed to cDNA with the TaqMan reverse transcription reagents (Applied Biosystems), and used to quantitatively amplify cDNA in real-time PCR in triplicate with the SYBR Green PCR Master Mix (Applied Biosystems) and a primer pair described before (53). Associated Gas5 RNA was shown as fold precipitations compared to the baseline, obtained with coprecipitation with control antibody or in the presence of control plasmid transfection in the absence of dexamethasone (Fig. 2A, middle panel; and Fig, 2C right panel). Gas5 was also detected with regular PCR employing an adjusted PCR cycle and a primer pair that amplifies the entire Gas5 sequence (Fig. 2BA, C, and 8F left panel). The amount of ncRNA of the transfected Gas5 fragments were also quantitatively evaluated in triplicate using SYBR Green real-time PCR with the forward primer: 5′-TTGGTACCGAGCTCGGATC-3′, which encodes the pcDNA3 sequence located 5′ terminally to the subcloned Gas5 sequence and is thus transcribed with Gas5 RNA, and reverse primers set in the Gas5 sequence; 5′-CCATAAGGTGCTATCCAGAGC-3′ for Gas5(1-598), (1-201) and (1-402); 5′-CAAGCCGACTCTCCATACC-3′ for Gas5(199-402) and (199-598); or 5′-CTCTAGCTTGGGTGAGGCAAG-3′ for Gas5(400-598). These primer pairs all produce Gas5 cDNA fragments with ~100 bps length. Entire sequences of endogenous Gas5, miR191, SC35, *t*RNA(Arg) and U75 snoRNA were also amplified in the regular PCR with adjusted PCR cycles by using the primer pair (Gas5: forward: 5′-CTTTTCGAGGTAGGAGTC-3′, reverse: 5′-AGACACTGTTTTAATCTTC-3′, fragment length: 598 bps; miR191: forward: 5′-CGGCTGGACAGCGGGCAAC-3′, reverse: 5′-AGGCAGGAGAGCAGGGGACGAAATC-3′, fragment length: 92 bps; SC35: forward: 5′-GATGTGGAGGGTATGAC-3′, reverse: 5′-CCTTCCTCTTCAGGAGAC-3′, fragment length: 626 bps; *t*RNA(Arg): 5′-GGACCACGTGGCCTAATG-3′, reverse: 5′-AACCACGAAGGGATTC-3′, fragment length: 73 bps). Primers for the SYBR Green real-time PCR (Table 1) were used for amplifying U75 snoRNA in this assay (fragment size: 56 bps).

RNA fluorescent in situ hybridization

HeLa cells were cultured in 2-well slide chambers and were fixed in 4% formaldehyde and permeabilized with 70% ethanol at 4°C overnight. After rehydration with 2× SCC containing 50% formamide, cells were hybridized at 37°C overnight in a mixture containing 10% dextran sulfate, 2 mM vanadyl-ribonucleoside complex, 0.02% BSA, 40 μg yeast *t*RNA, 2× SSC, 50% formamide, and 30 ng of the Alexa488-conjugated Gas 5 probe (GTGCTATCCAGAGCCACACTGCATCTGCACCCAGCACCATACCTCACAG) (Invitrogen, Palo Alto, CA). After washing with 2× and 0.1× SCC with 50% formamide, slides were mounted with the Vectashield with DAPI (4,6-diamidino-2-phenylindole) (Vector Laboratories, Inc., Burlingame, CA) and were examined under the Zeiss LSM510 meta/Zeiss axiovert 200M microscope stand (Carl Zeiss MicroImaging, Inc., Thornwood, NY) at the NICHD Microscopy & Imaging Core (National Institute of Child Health and Human Development, Bethesda, MD) with the assistance of Dr. Vincent Schram.

Subcellular fractionation and Western blots

Subcellular fractionations were carried out as previously reported (51). Briefly, HeLa cells were treated with 10^{-6} M of dexamethasone or vehicle for 3 hours. They were then harvested and homogenated in buffer containing 50 mM Tris-HCl [pH 7.4], 25 mM KCl, 5 mM $MgCl_2$, 0.5 mM dithiothreitol, 0.25 M sucrose, 1 Tab/50 ml Complete™ Tablet (Roche Applied

Bioscience), and 1 U/μl of the RNase inhibitor RNAsin (Promega), and were centrifuged at 500*g* for 5 min to obtain the whole homogenate. All the procedures were carried out at 4°C. The whole homogenates were then centrifuged at 2,000*g* for 15 min to harvest the nuclear fraction (pellet) and the supernatant was further centrifuged at 105,000*g* for 1 hour to harvest the cytoplasmic fraction (supernatant). The nuclear fraction was washed once with the same buffer. Using aliquots of the nuclear and cytoplasmic fractions, total RNA was purified and Gas5 abundance was determined using the SYBR Green real-time PCR as described above. Aliquots of samples (10 μg protein) were also run on SDS-PAGE gels, transferred to the nitrocellulose membranes, and GR, α-tubulin, and Oct1 were detected with their specific antibodies (Santa Cruz Biotechnology, Inc.). To evaluate the abundance of GR and G-gal-G, aliquots of samples were separated on SDS-PAGE gels, blotted, and visualized with a GR antibody raised against GR LBD (Affinity Bioreagents).

Chromatin-immunoprecipitation (ChIP) assays

ChIP assays were performed in HeLa and HepG2 cells, as previously described (53). They were transfected with Gas5-expressing plasmids using the Nucleofector system, and were exposed to either 10^{-6} M of dexamethasone, 10^{-6} M of GW501516, or corresponding vehicles for 8 hours. They were then fixed, DNA and bound proteins were cross-linked, and ChIP assays were performed by coprecipitating the DNA/protein complexes with a GR antibody (Affinity Bioreagents), a PPARδ antibody (Santa Cruz Biotechnologies, Inc.), or rabbit control IgG (Santa Cruz Biotechnology, Inc.). Aliquots of suspended cells were used for purifying total RNA before fixation for some experiments. The promoter regions of the ADRP, cIAP2, G6Pase, GILZ, PEPCK, and SGK1, which contain PPREs or GREs were amplified from the prepared DNA samples using the primer pairs shown in Table 2 in the SYBR Green real-time PCR, in the regular PCR with adjusted PCR cycles, or in both. Products of the regular PCRs were run on 3% agarose gels.

Thymidine incorporation assay

HeLa cells transfected with Gas5 or control siRNA were cultured in serum-free medium for indicated periods and were treated with 10^{-6} M of dexamethasone for 24 hours. 2 μCi of [^{3}H] thymidine (MP Biologicals, Irvine, CA) was then added to the medium and the cells were cultured for an additional 4 hours. The cells were harvested and washed with PBS several times and associated radioactivity was counted with the Bechman LS6000IC counter (Beckman Coulter, Inc., Fullerton, CA). Counted radioactivity was corrected for total RNA concentrations and percentage over the baseline was shown in Fig. 6A. In this figure, thymidine incorporation into the cells gradually decreased during the time of the incubation, indicating that a progressively increasing number of these cells stopped growing.

TUNEL and caspase assays

HeLa cells were transfected with Gas5 or control siRNA and were incubated with serum-free medium for 72 hours. The cells were then incubated with 10^{-6} M of dexamethasone, 250 U/ml of IFNγ, and 100 ng/ml of Fas antibody for 24 hours. They were then fixed and apoptotic cells were labeled with the MEBSTAIN Apoptosis *TUNEL* Kit Direct (MBL International Corporation, Inc., Woburn, MA). Over 200 cells were counted in three different experiments and apoptotic cells were expressed as percentage over the total cells. For caspase assays, HeLa cells were seeded at 0.5×10^{4} cells/well in 96-well plates, transfected with Gas5 or siRNA, and incubated with serum-free medium for 72 hours. They were then incubated with 10^{-6} M of dexamethasone, 250 U/ml of IFNγ and 100 ng/ml of Fas antibody for 24 hours. Activities of caspase 3 or 7 (3/7) and 9 were directly measured by adding reaction mixtures provided by the Caspase-Glo 3/7 and 9 assay kits (Promega) into each well and by measuring the luminescence activity after 30 min of incubation using the GloMax Luminometer (Promega).

In vitro binding assay

Bacterially produced and GST bead-associated GST, GST-fused wild type GR DBD and its mutants harboring K442A, R447A, or both mutations were mixed with RNA of the wild type Gas5, GRE-1 Mut, GRE-2 Mut, or GRE-1/2 Mut Helix produced with the RiboMax Large Scale RNA Production System (Promega) in buffer containing 50 mM Tris-HCl (pH 8.0), 50 mM NaCl, 1 mM EDTA, 0.1 % NP-40, 10 % glycerol, 1u/μl RNase inhibitor RNAsin (Promega), and 0.1 mg/ml BSA at 4°C for 20 min. After vigorous washing with the buffer, associated Gas5 RNAs were purified with TRIZOL™ reagent (Invitrogen), reverse transcribed to cDNA with the TaqMan reverse transcription reagents (Applied Biosystems), and were finally amplified in SYBR Green real-time PCR using the primer pair as described above. For competition assays, double-stranded DNA GREs in the presence or absence of FAM-modification (Invitrogen) (sense wild type GRE: 5′-AGAGGATCTGTACAGGATGTTCTAGAT-3′, sense mutant GRE: 5′-AGAGGATCT**C**TACAGGAT**C**TTCTAGAT-3′: GREs are indicated with underline) were produced by annealing with their corresponding antisense oligonucleotides and added to the reactions. The amount of FAM-labeled DNA GRE associated with GST-GR DBD was measured with the Victor 3 (Applied Biosystems) with the F485 and F535 as an excitation and an emission filter, respectively. For binding assays, indicated concentrations of Gas5 RNAs were incubated with 1μg of GST-GR DBD bound on GST beads and associated Gas5 RNA was examined with SYBR Green real-time PCR. Scatchard analyses were performed using the GraphPad PRISM® 4 software (GraphPad Software Inc., San Diego, CA). Competition assays examining association of FAM-labeled double-stranded DNA GREs to 1μg of GST-GR DBD were performed in the presence of increasing concentrations of non-labeled double-stranded DNA GREs, wild type Gas5 or Gas5 GRE-1 Mut RNAs.

Statistical analysis

Statistical analysis was carried out by unpaired Student *t* test with the two-tailed P value.

Supplementary Material

Refer to Web version on PubMed Central for supplementary material.

Acknowledgments

This study was funded by the Intramural Research Program of the *Eunice Kennedy Shriver* National Institute of Child Health and Human Development and the National Institute of Allergy and Infectious Diseases, National Institutes of Health, Bethesda, MD. We thank Drs. R.M. Evans, F. French, G.L. Hager, Y. Shi, S.S. Simons Jr., J.A. Steitz, M-J. Tsai, B. Vogelstein and N. Warriar for providing their plasmids, Drs. R.J. Maraia and A. Porras for helpful discussion on the RNA fluorescent *in situ* hybridization and M.K. Zachman for his superb technical assistance.

References and notes

1. Lopez-Maury L, Marguerat S, Bahler J. Tuning gene expression to changing environments: from rapid responses to evolutionary adaptation. Nat Rev Genet 2008;9:583–593. [PubMed: 18591982]
2. Sellick CA, Reece RJ. Eukaryotic transcription factors as direct nutrient sensors. Trends Biochem Sci 2005;30:405–412. [PubMed: 15950477]
3. Kino, T.; Chrousos, GP. Glucocorticoid Effect on Gene Expression. In: Steckler, T.; Kalin, NH.; Reul, JMHM., editors. Handbook on Stress and the Brain Part 1. Elsevier BV; Amsterdam: 2004. p. 295-312.
4. Chrousos, GP. Glucocorticoid therapy. In: Felig, P.; Frohman, LA., editors. Endocrinology & Metablism. McGraw-Hill; New York: 2001. p. 609-632.
5. Chrousos GP, Kino T. Intracellular glucocorticoid signaling: a formerly simple system turns stochastic. Sci STKE 2005 2005:pe48.

6. Frankfurt O, Rosen ST. Mechanisms of glucocorticoid-induced apoptosis in hematologic malignancies: updates. Curr Opin Oncol 2004;16:553–563. [PubMed: 15627017]
7. Wen LP, Madani K, Fahrni JA, Duncan SR, Rosen GD. Dexamethasone inhibits lung epithelial cell apoptosis induced by IFN-γ and Fas. Am J Physiol 1997;273:L921–929. [PubMed: 9374718]
8. Kino T, De Martino MU, Charmandari E, Mirani M, Chrousos GP. Tissue glucocorticoid resistance/hypersensitivity syndromes. J Steroid Biochem Mol Biol 2003;85:457–467. [PubMed: 12943736]
9. Abel GA, et al. Activity of the GR in G2 and mitosis. Mol Endocrinol 2002;16:1352–1366. [PubMed: 12040020]
10. Cidlowski JA, Michaels GA. Alteration in glucocorticoid binding site number during the cell cycle in HeLa cells. Nature 1977;266:643–645. [PubMed: 859631]
11. Chrousos GP, Kino T. Glucocorticoid action networks and complex psychiatric and/or somatic disorders. Stress 2007;10:213–219. [PubMed: 17514590]
12. Kino T, Chrousos GP. Glucocorticoid and mineralocorticoid receptors and associated diseases. Essays Biochem 2004;40:137–155. [PubMed: 15242344]
13. Mattick JS. The functional genomics of noncoding RNA. Science 2005;309:1527–1528. [PubMed: 16141063]
14. Barrandon C, Spiluttini B, Bensaude O. Non-coding RNAs regulating the transcriptional machinery. Biol Cell 2008;100:83–95. [PubMed: 18199047]
15. Schneider C, King RM, Philipson L. Genes specifically expressed at growth arrest of mammalian cells. Cell 1988;54:787–793. [PubMed: 3409319]
16. Coccia EM, et al. Regulation and expression of a growth arrest-specific gene (gas5) during growth, differentiation, and development. Mol Cell Biol 1992;12:3514–3521. [PubMed: 1630459]
17. Smith CM, Steitz JA. Classification of gas5 as a multi-small-nucleolar-RNA (snoRNA) host gene and a member of the 5′-terminal oligopyrimidine gene family reveals common features of snoRNA host genes. Mol Cell Biol 1998;18:6897–6909. [PubMed: 9819378]
18. Amaldi, F.; Pierandrei-Amaldi, P. TOP genes: a translationaly controlled class of genes including those coding for ribosomal proteins. In: Jeanteur, P., editor. Progress in molecular and subcellular biology. Vol. 18. Springer-Verlag; Berlin, Germany: 1997. p. 1-17.
19. Hatchell EC, et al. SLIRP, a small SRA binding protein, is a nuclear receptor corepressor. Mol Cell 2006;22:657–668. [PubMed: 16762838]
20. Lanz RB, et al. A steroid receptor coactivator, SRA, functions as an RNA and is present in an SRC-1 complex. Cell 1999;97:17–27. [PubMed: 10199399]
21. Rosenfeld MG, Lunyak VV, Glass CK. Sensors and signals: a coactivator/corepressor/epigenetic code for integrating signal-dependent programs of transcriptional response. Genes Dev 2006;20:1405–1428. [PubMed: 16751179]
22. Ali M, Vedeckis WV. The glucocorticoid receptor protein binds to transfer RNA. Science 1987;235:467–470. [PubMed: 3798121]
23. Savory JG, et al. Discrimination between NL1- and NL2-mediated nuclear localization of the glucocorticoid receptor. Mol Cell Biol 1999;19:1025–1037. [PubMed: 9891038]
24. Webster JC, et al. Dexamethasone and tumor necrosis factor-α act together to induce the cellular inhibitor of apoptosis-2 gene and prevent apoptosis in a variety of cell types. Endocrinology 2002;143:3866–3874. [PubMed: 12239098]
25. Hong SY, et al. Involvement of two NF-κB binding elements in tumor necrosis factor α-, CD40-, and epstein-barr virus latent membrane protein 1-mediated induction of the cellular inhibitor of apoptosis protein 2 gene. J Biol Chem 2000;275:18022–18028. [PubMed: 10751398]
26. Deveraux QL, Reed JC. IAP family proteins--suppressors of apoptosis. Genes Dev 1999;13:239–252. [PubMed: 9990849]
27. Asselin-Labat ML, et al. GILZ, a new target for the transcription factor FoxO3, protects T lymphocytes from interleukin-2 withdrawal-induced apoptosis. Blood 2004;104:215–223. [PubMed: 15031210]
28. Itani OA, Liu KZ, Cornish KL, Campbell JR, Thomas CP. Glucocorticoids stimulate human sgk1 gene expression by activation of a GRE in its 5′-flanking region. Am J Physiol Endocrinol Metab 2002;283:E971–979. [PubMed: 12376324]

29. Wang XL, et al. The synergistic effect of dexamethasone and all-trans-retinoic acid on hepatic phosphoenolpyruvate carboxykinase gene expression involves the coactivator p300. J Biol Chem 2004;279:34191–34200. [PubMed: 15166231]
30. Vander Kooi BT, et al. The glucose-6-phosphatase catalytic subunit gene promoter contains both positive and negative glucocorticoid response elements. Mol Endocrinol 2005;19:3001–3022. [PubMed: 16037130]
31. Tachibana K, et al. Gene expression profiling of potential peroxisome proliferator-activated receptor (PPAR) target genes in human hepatoblastoma cell lines inducibly expressing different PPAR isoforms. Nucl Recept 2005;3:3. [PubMed: 16197558]
32. Mikosz CA, Brickley DR, Sharkey MS, Moran TW, Conzen SD. Glucocorticoid receptor-mediated protection from apoptosis is associated with induction of the serine/threonine survival kinase gene, sgk-1. J Biol Chem 2001;276:16649–16654. [PubMed: 11278764]
33. Cardone MH, et al. Regulation of cell death protease caspase-9 by phosphorylation. Science 1998;282:1318–1321. [PubMed: 9812896]
34. Dimitrov RA, Zuker M. Prediction of hybridization and melting for double-stranded nucleic acids. Biophys J 2004;87:215–226. [PubMed: 15240459]
35. Varani G, McClain WH. The G.U wobble base pair. A fundamental building block of RNA structure crucial to RNA function in diverse biological systems. EMBO Rep 2000;1:18–23. [PubMed: 11256617]
36. Luisi BF, et al. Crystallographic analysis of the interaction of the glucocorticoid receptor with DNA. Nature 1991;352:497–505. [PubMed: 1865905]
37. Rundlett SE, Miesfeld RL. Quantitative differences in androgen and glucocorticoid receptor DNA binding properties contribute to receptor-selective transcriptional regulation. Mol Cell Endocrinol 1995;109:1–10. [PubMed: 7789609]
38. Markham NR, Zuker M. UNAFold: software for nucleic acid folding and hybridization. Methods Mol Biol 2008;453:3–31. [PubMed: 18712296]
39. Das R, Baker D. Automated de novo prediction of native-like RNA tertiary structures. Proc Natl Acad Sci U S A 2007;104:14664–14669. [PubMed: 17726102]
40. Schena M, Freedman LP, Yamamoto KR. Mutations in the glucocorticoid receptor zinc finger region that distinguish interdigitated DNA binding and transcriptional enhancement activities. Genes Dev 1989;3:1590–1601. [PubMed: 2515114]
41. Willkomm DK, Hartmann RK. 6S RNA - an ancient regulator of bacterial RNA polymerase rediscovered. Biol Chem 2005;386:1273–1277. [PubMed: 16336121]
42. Barthel A, Schmoll D. Novel concepts in insulin regulation of hepatic gluconeogenesis. Am J Physiol Endocrinol Metab 2003;285:E685–692. [PubMed: 12959935]
43. Mourtada-Maarabouni M, Pickard MR, Hedge VL, Farzaneh F, Williams GT. GAS5, a non-protein-coding RNA, controls apoptosis and is downregulated in breast cancer. Oncogene 2009;28:195–208. [PubMed: 18836484]
44. Haywood ME, et al. Overlapping BXSB congenic intervals, in combination with microarray gene expression, reveal novel lupus candidate genes. Genes Immun 2006;7:250–263. [PubMed: 16541099]
45. Franceschi RT. Interaction of the 1α,25-dihydroxyvitamin D3 receptor with RNA and synthetic polyribonucleotides. Proc Natl Acad Sci U S A 1984;81:2337–2341. [PubMed: 6201853]
46. Lino S, et al. RNA-dependent release of androgen and other steroidreceptor complexes from DNA. J Biol Chem 1980;255:5545–5551. [PubMed: 6155376]
47. Chong MT, Lippman ME. Effects of RNA and ribonuclease on the binding of estrogen and glucocorticoid receptors from MCF-7 cells to DNA-cellulose. J Biol Chem 1982;257:2996–3002. [PubMed: 7061461]
48. Leygue E. Steroid receptor RNA activator (SRA1): unusual bifaceted gene products with suspected relevance to breast cancer. Nucl Recept Signal 2007;5:e006. [PubMed: 17710122]
49. De Martino MU, et al. The glucocorticoid receptor and the orphan nuclear receptor chicken ovalbumin upstream promoter-transcription factor II interact with and mutually affect each other's transcriptional activities: implications for intermediary metabolism. Mol Endocrinol 2004;18:820–833. [PubMed: 14739255]

50. Kino T, et al. Cyclin-dependent kinase 5 differentially regulates the transcriptional activity of the glucocorticoid receptor through phosphorylation: clinical implications for the nervous system response to glucocorticoids and stress. Mol Endocrinol 2007;21:1552–1568. [PubMed: 17440046]

51. Kino T, et al. G protein β interacts with the glucocorticoid receptor and suppresses its transcriptional activity in the nucleus. J Cell Biol 2005;169:885–896. [PubMed: 15955845]

52. Kino T, et al. The HIV-1 virion-associated protein vpr is a coactivator of the human glucocorticoid receptor. J Exp Med 1999;189:51–62. [PubMed: 9874563]

53. Ichijo T, et al. The Smad6-histone deacetylase 3 complex silences the transcriptional activity of the glucocorticoid receptor: potential clinical implications. J Biol Chem 2005;280:42067–42077. [PubMed: 16249187]

54. Mourtada-Maarabouni M, Hedge VL, Kirkham L, Farzaneh F, Williams GT. Growth arrest in human T-cells is controlled by the non-coding RNA growth-arrest-specific transcript 5 (GAS5). J Cell Sci 2008;121:939–946. [PubMed: 18354083]

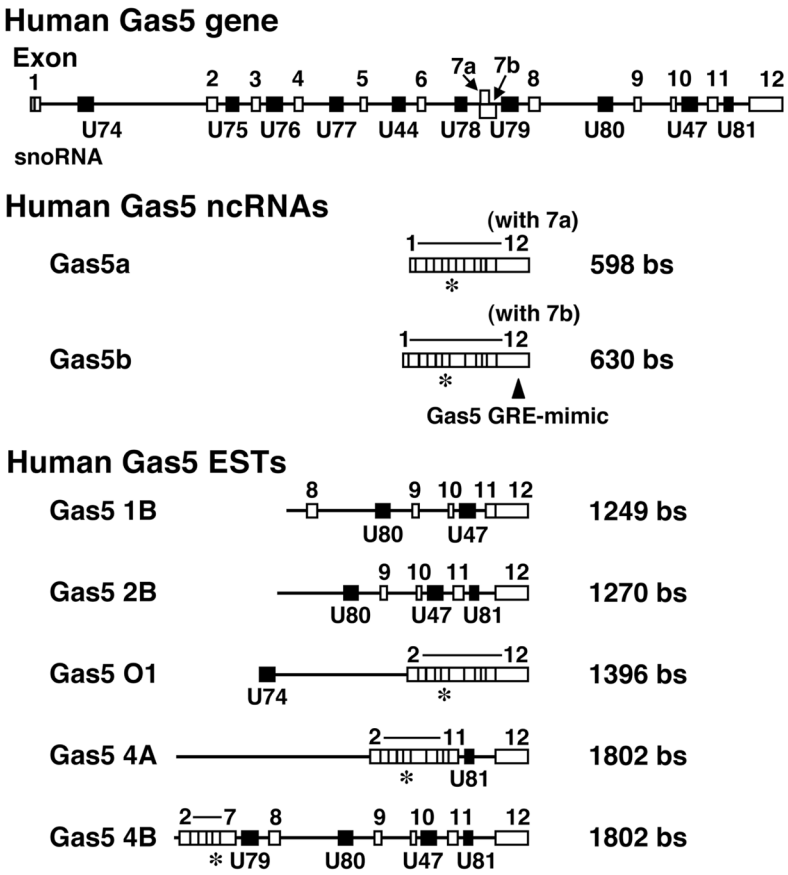

Fig. 1. The organization of the Gas5 gene and its ncRNA products

The human Gas5 gene contains 12 exons (white boxes) and 10 snoRNAs (black boxes), and produces two mature, spliced isoforms Gas5a and Gas5b with alternative use of exon 7a and b, in addition to at least 5 other variants reported as ESTs, which contain one or more snoRNA sequences (Genbank accession number NR_002578 and AF141346) (17,54). Gray box located 5′ terminally to exon 1 indicates 5′TOP sequence. In our study, we called Gas5a as Gas5 and studied its expression and effects, as this isoform is the main form expressed in HeLa cells. The Gas5 siRNA we employed corresponds to a sequence located in exon 6 and its location in Gas5 isoforms is shown with "*". Gas5 GRE-mimic is located in exon 12, which is found in all splicing isoforms. bs: bases, EST: expression sequence tag, GRE: glucocorticoid response element, ncRNA: noncoding RNA, snoRNA: small nucleolar RNA.

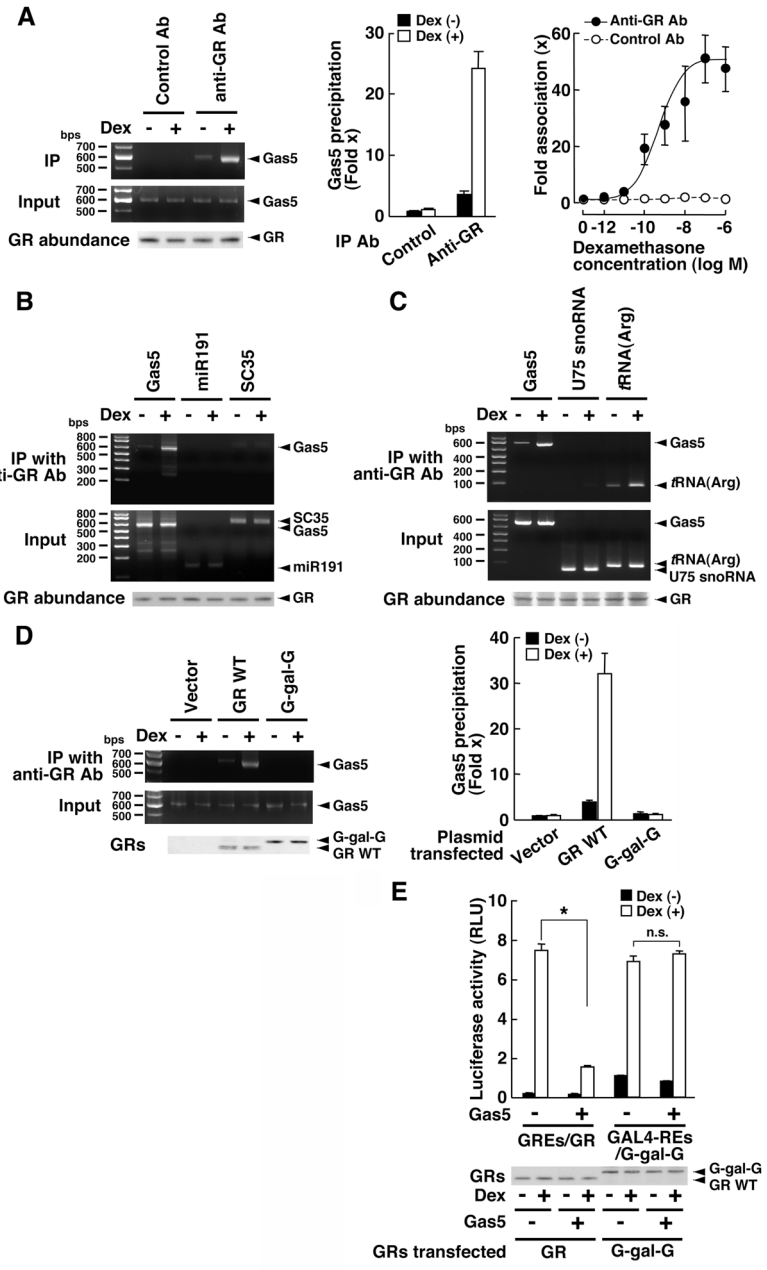

Fig. 2. Gas5 RNA interacts with GR at its DBD and suppresses its transcriptional activity

(A) Endogenous Gas5 interacts with GR in a dexamethasone-dependent fashion. GR-expressing HeLa cells were treated with 10^{-6} M of dexamethasone. The GR/RNA complex was precipitated with a specific antibody against GR LBD (anti-GR Ab), and rabbit IgG was used as a negative control. GR-associated Gas5 was detected with regular PCR (left panel) employing an adjusted PCR cycle and a primer pair that amplifies the entire Gas5 sequence or with SYBR Green real-time PCR (middle panel) using a specific primer pair. Results of Western blots show the abundance of the GR protein (bottom gel of the left panel). The right panel shows titration curves of dexamethasone for the association of Gas5 to GR examined with anti-GR (closed circles) or control (open circles) antibody. Bars and circles represent the mean +/− SEM values of the fold Gas5 precipitation over the baseline ("Control" in the absence of dexamethasone) (n=3). IP Ab: antibody used for immunoprecipitation. **(B, C)** GR is

associated with Gas5 and *t*RNA(Arg) in a ligand-dependent fashion, whereas control RNAs miR191, SC35 mRNA, and U75 snoRNA are not. HeLa cells were treated with 10^{-6} M of dexamethasone. GR-associated Gas5, miR191, and SC35 mRNA (**B**), or U75 snoRNA and *t*RNA(Arg) mRNA (**C**) were detected with regular PCR employing an adjusted PCR cycle and specific primer pairs that amplify the entire sequences. Results of Western blots demonstrating GR protein abundance are shown in the bottom gels. **(D)** Gas5 is associated with the GR DBD. GR-deficient HCT116 cells were transfected with the control plasmid (Vector), pRShGRα (GR WT), or G-gal-G, and treated with 10^{-6} M of dexamethasone. Gas5 coprecipitated with GR or G-gal-G with a GR LBD-specific antibody (anti-GR Ab) was detected with regular PCR (left panel) employing an adjusted PCR cycle and a primer pair that amplifies the entire Gas5 sequence or with SYBR Green real-time PCR (right panel) using a specific primer pair. Western blots showing the abundance of GR WT and G-gal-G are provided at the bottom of the left panel. Bars represent the mean +/− SEM values of fold Gas5 precipitation over the baseline ("Vector" in the absence of dexamethasone) (n=3). IP: immunoprecipitation. **(E)** Gas5 suppresses the transcriptional activity of wild type (WT) GR but not of the GR chimera containing the GAL4 DBD. HCT116 cells were transfected with the Gas5-expressing plasmid together with pRShGRα and pMMTV-Luc, or G-gal-G and p17mer-tk-Luc, in the presence of pSV40-β-Gal. Western blots showing GR WT and G-gal-G abundance are provided at the bottom. Bars represent the mean +/− SEM values of luciferase activity normalized to β-galactosidase activity. *; $p<0.01$; n.s., not significant, compared to the baseline (in the presence of control siRNA and dexamethasone) (n=3).

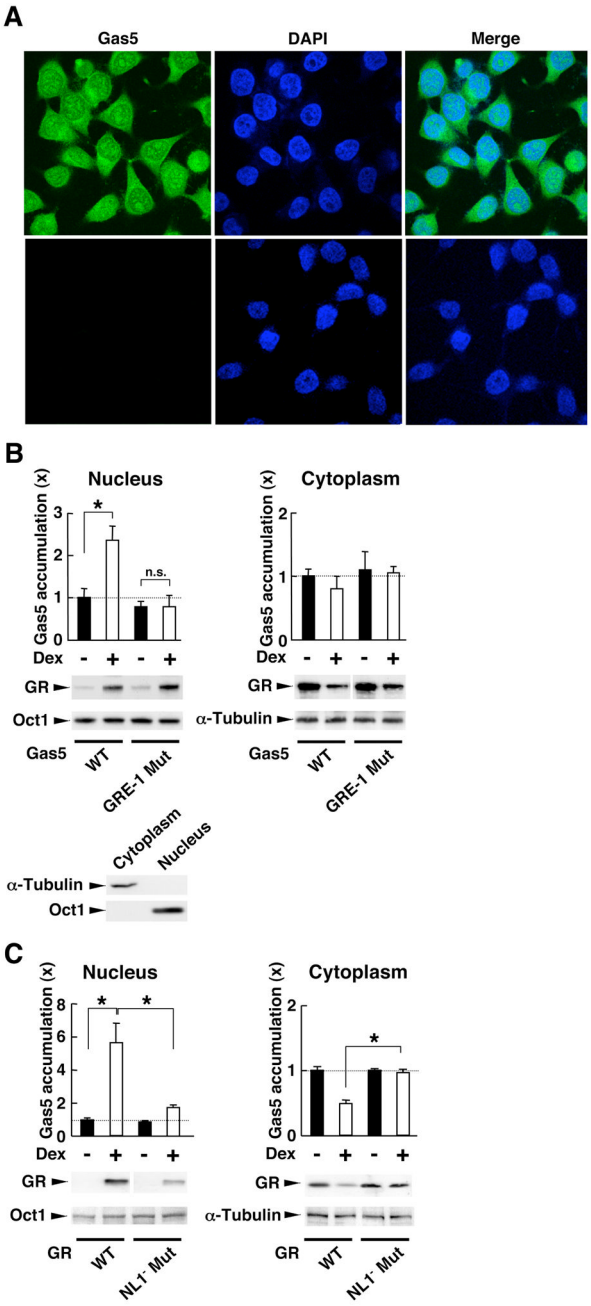

Fig. 3. Gas5 is located both in the cytoplasm and the nucleus and translocates from the cytoplasm into the nucleus with GR in response to dexamethasone

(A) Gas5 is localized both in the cytoplasm and the nucleus. Top left shows RNA fluorescence in situ hybridization performed with the Alexa488-labeled Gas5 probe in HeLa cells. Bottom left shows the negative control obtained with samples treated with RNase. Middle panels demonstrate staining with DAPI, and the right panels show merged images of left and middle panels. **(B)** Gas5 translocates into the nucleus with GR in response to dexamethasone. HeLa cells were transfected with Gas5 wild type (WT)- or GRE-1 Mut-expressing plasmid and were treated with 10^{-6} M of dexamethasone. Transfected Gas5s and endogenous GR, α-tubulin, and Oct1 in these subcellular fractions were detected with SYBR Green real-time PCR and Western blots, respectively (top panels). The bottom panel shows Western blots for the presence of α-

tubulin and Oct1 in the subcellular fractions. To detect exogenously expressed Gas5, we employed the forward primer, which recognized the plasmid sequence adjacent to 5′ end of the Gas5 sequence that was expressed with Gas5 RNA. Bars represent the mean +/− SEM values of fold accumulation of Gas5 RNA compared to the baseline (transfected with wild type Gas5 RNA in the absence of dexamethasone). *: $p<0.01$, compared to the conditions indicated (n=3). **(C)** The GR mutant defective in nuclear translocation reduces cytoplasmic to nuclear translocation of Gas5. GR-deficient HCT116 cells were transfected with GR WT- or NL1^{-} mutant-expressing plasmid and were treated with 10^{-6} M of dexamethasone. Endogenous Gas5 and transfected GRs, α-tubulin, and Oct1 in these subcellular fractions were detected with SYBR Green real-time PCR and Western blots, respectively. Bars represent the mean +/− SEM values of fold accumulation of Gas5 RNA compared to the baseline (transfected with wild type GR in the absence of dexamethasone) (n=3).

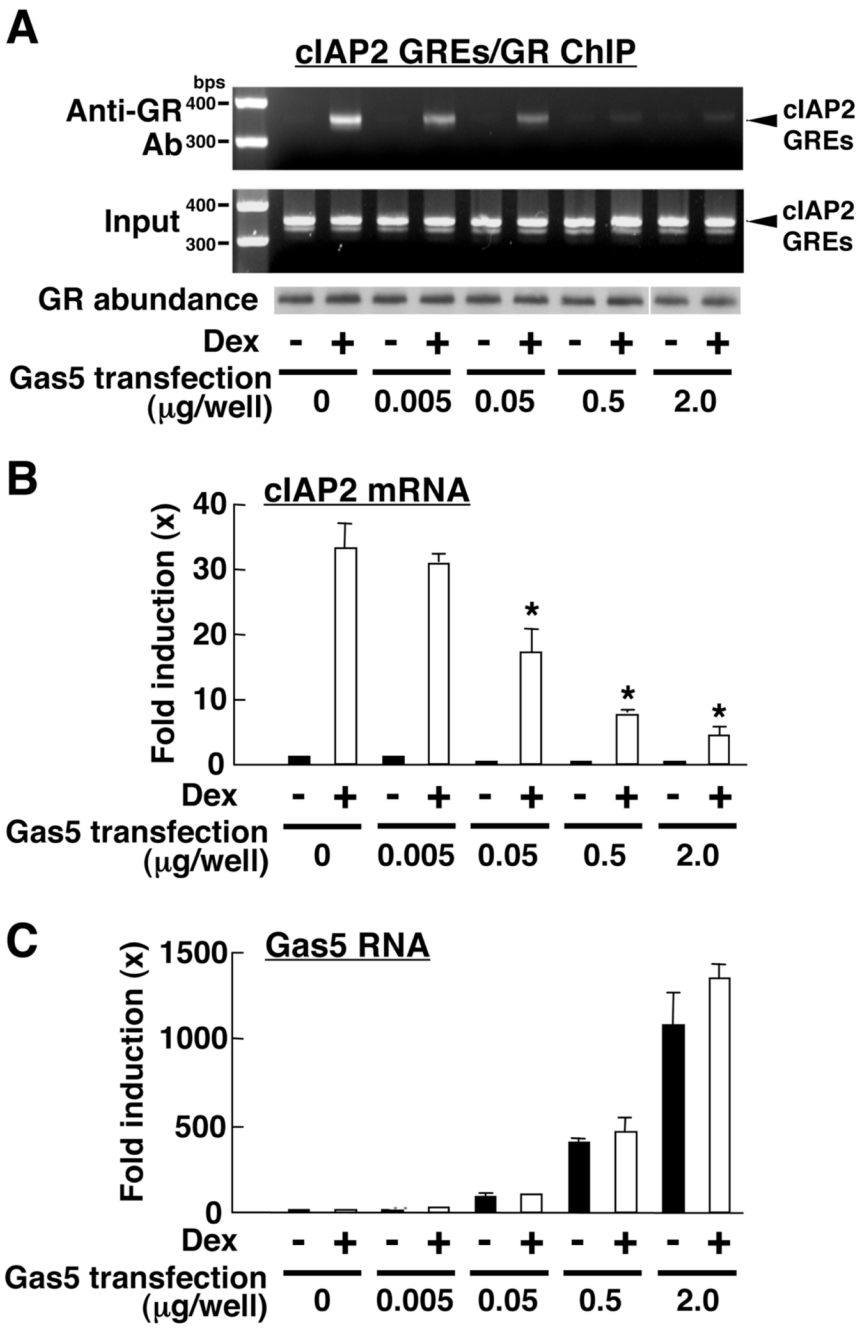

Fig. 4. Overexpression of Gas5 suppresses both the association of GR with cIAP2 GREs and GR-induced *cIAP2* mRNA expression

HeLa cells were transfected with increasing amounts of Gas5-expressing plasmid and treated with 10^{-6} M of dexamethasone. The ChIP assay and total RNA purification were performed using fractions of these cells. **(A)** Gas5 suppresses the association of GR with *cIAP2* GREs. ChIP assays were performed with the GR antibody against GR LBD (anti-GR Ab) and the *cIAP2* promoter fragment that contains tandem GREs was amplified by PCR with an adjusted PCR cycle using a specific primer pair. The bottom blots are Western blots showing GR protein abundance.

(B and C) Gas5 suppresses dexamethasone-induced *cIAP2* mRNA expression. Total RNA was purified, and the abundance of the *cIAP2* and control *RPLP0* mRNAs and of the Gas5 RNA were measured with SYBR Green real-time PCR. Bars represent the mean +/− SEM values of fold induction of the *cIAP2* mRNA (B) and the Gas5 RNA (C) expression normalized for the *RPLP0* mRNA abundance compared to the baseline (in the absence of Gas5 transfection and dexamethasone). *, $p < 0.01$, compared to the condition in the absence of Gas5 transfection and in the presence of dexamethasone (n=3).

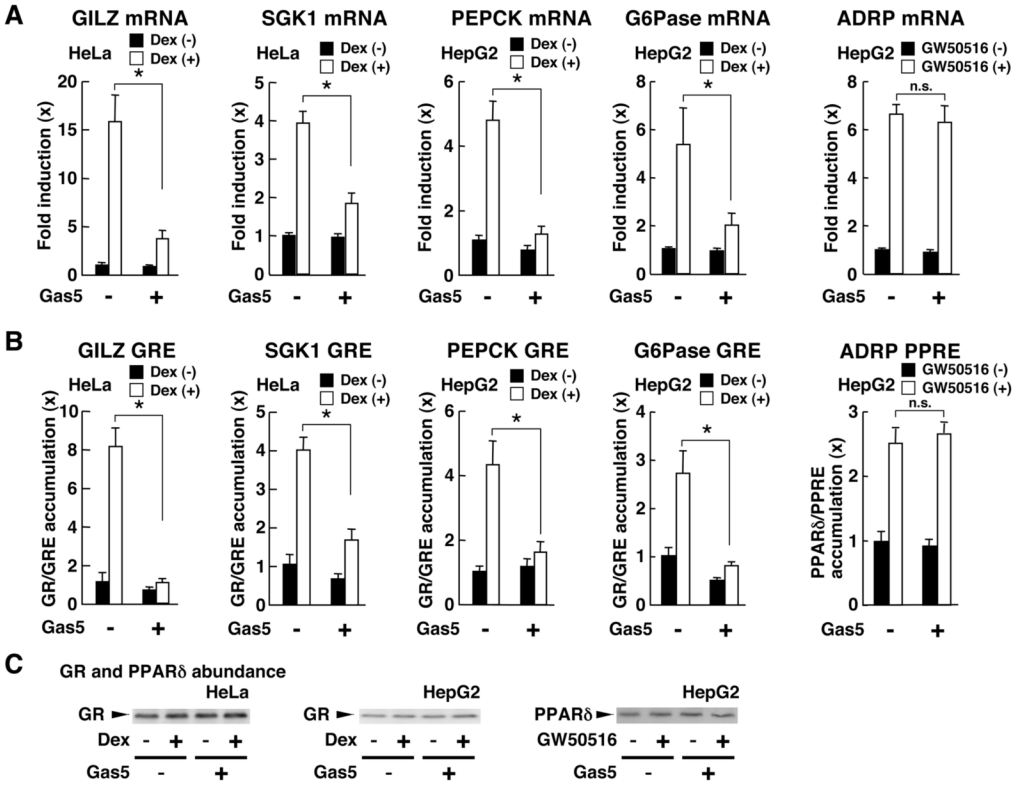

Fig. 5. Gas5 suppresses GR-induced mRNA expression of glucocorticoid-responsive genes, as well as the association of GR to their GREs, but does not influence PPARδ-induced mRNA expression of the *ADRP* gene or the association of PPARδ to its PPREs

HeLa and HepG2 cells were transfected with the Gas5-expressing plasmid and treated with 10^{-6}M of dexamethasone or GW501516. Total RNA purification, ChIP assays, and Western blots were performed from the appropriate samples. mRNA abundance of the glucocorticoid-responsive genes encoding GILZ, SGK1, PEPCK, and G6Pase, and the PPARδ-responsive gene *ADRP* (**A**), as well as the association of GR and PPARδ to their GREs or PPREs in ChIP assays (**B**) were examined with SYBR Green real-time PCR with their specific primer pairs. Bars represent the mean +/− SEM values of fold mRNA expression (**A**) and fold association of GR and PPARδ to their GREs or PPREs (**B**) compared to the baseline (in the absence of Gas5 transfection and dexamethasone or GW501516 treatment). *: $p<0.01$, n.s.: not significant, compared to the conditions indicated (n=3). (**C**) The abundance of GR and PPARδ was analyzed by Western blotting.

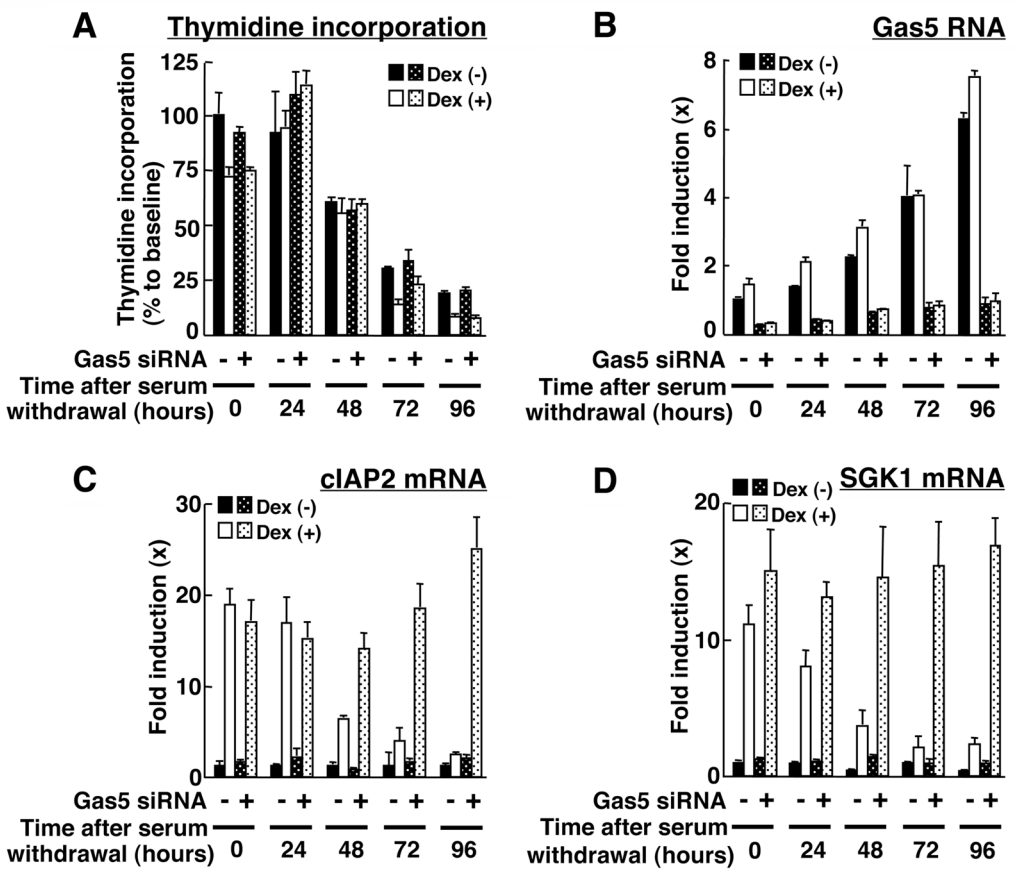

Fig. 6. Endogenous Gas5 functions as a negative regulator of GR-induced *cIAP2* and *SGK1* mRNA expression

HeLa cells were transfected with Gas5 or control siRNA and were cultured in serum-free medium for the indicated time periods. The abundance of the *cIAP2*, *SGK1*, and RPLP0 mRNAs and of the Gas5 RNA were determined with SYBR Green real-time PCR. (**A**) Thymidine incorporation was also examined in cells from the same experiment and is shown as % of the baseline. Bars represent the mean +/− SEM values of fold induction of the Gas5 RNA (**B**) and the cIAP2 (**C**) and SGK1 (**D**) mRNAs normalized for *RPLP0* mRNA abundance compared to the baseline (in the absence of Gas5 siRNA and dexamethasone at time “0”). (n=3).

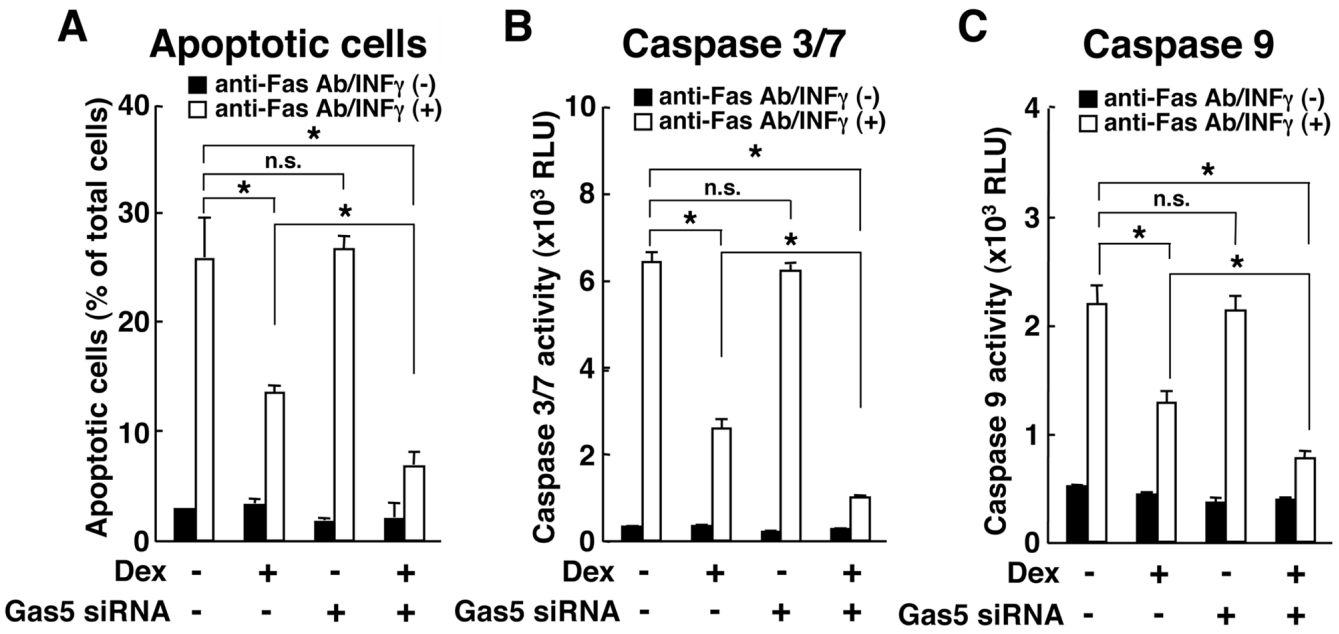

Fig. 7. Depletion of endogenous Gas5 with siRNA potentiated dexamethasone-induced inhibition of apoptosis and caspase activities caused by treatment with Fas antibody and IFN-γ

HeLa cells were transfected with Gas5 or control siRNA and cultured in serum-free medium for 72 hours. 10^{-6} M of dexamethasone, 100 ng/ml of Fas antibody (anti-Fas Ab), and 250 U/ml of IFN-γ were added to the medium. (**A**) The percent of apoptotic cells. Bars represent the mean +/− SEM values of % of *TUNEL*-positive apoptotic cells in over 200 counted cells. The activities of caspase 3/7 (**B**) and 9 (**C**) are shown. Bars represent the mean +/− SEM values. *, $p<0.01$; n.s., not significant, compared to the condition indicated (n=3).

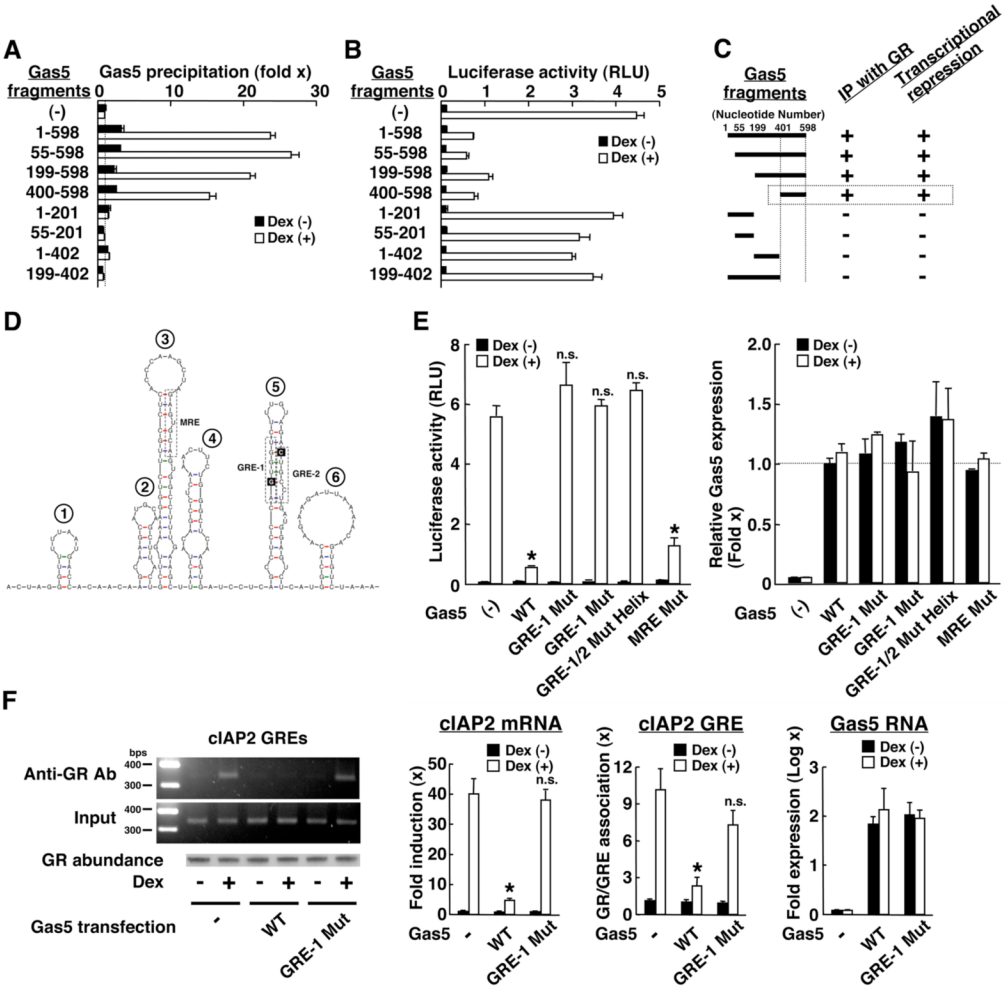

Fig. 8. Gas5 forms hairpin structures and interacts through its 3′ portion with the GR

(A) Gas5 is associated with GR through its nucleotides 400 to 598. HeLa cells were transfected with plasmids expressing the indicated fragments of Gas5 and treated with 10^{-6} M of dexamethasone and RNA/protein coprecipitation assays were performed. GR-associated Gas5 fragments were detected with SYBR Green real-time PCR. The forward primer recognizing the plasmid sequence adjacent to 5′ end of the Gas5 sequence and the reverse primers in the Gas5 sequence were used to amplify exogenously expressed Gas5 fragments. (**B**) Gas5 suppresses GR-induced transcriptional activity though nucleotides 400 to 598. HeLa cells were transfected with plasmids expressing the indicated fragments of Gas5 together with the GR-expressing plasmid, pMMTV-Luc, and pSV40-β-Gal. Bars represent the mean +/− SEM values of luciferase activity normalized for β-galactosidase activity (n=3). **(C)** Summary of functional and physical interactions between Gas5 and the GR. Results from the coimmunoprecipitation and reporter assays both indicate that Gas5 interacts with GR through the region enclosed by its nucleotides 400 to 598. IP, immunoprecipitation. (**D**) 2-dimensional structure of Gas5 nucleotides 400–598. Gas5 (400-598) consists of 6 hairpin structures and the hairpin #5 contains two “GRE” sequences at nucleotides 539–544 (“GRE-1”) and 553–559 (“GRE-2”) (shown in boxes), which form a double-stranded hairpin structure that we call the Gas5 GRE-mimic. Gas5 hairpin #3 harbors, at nucleotides 473–478, a MRE-resembling sequence, which does not have a perfectly complementing sequence. G540 and C554 of the Gas5 GRE-mimic, located at the 5′ and 3′ strands, respectively, are shown in black boxes. These residues are

conserved among the consensus DNA GREs and are critical for them to interact with K442 and R447 residues of the GR DBD to specify their affinity to this protein module (36). Wobble base-pairing is indicated in green, and Watson-Crick base-pairing is shown with blue and red. **(E)** Double-stranded GRE is required for Gas5 to repress GR-induced transcriptional activity. HCT116 cells were transfected with the indicated Gas5-expressing plasmid together with pRShGRα and pMMTV-Luc in the presence of pSV40-β-Gal. Luciferase activity is shown in the left panel, and RNA expression of Gas5 wild type (WT) and mutants measured with SYBR Green real-time PCR are shown in the right panel. Bars represent the mean +/− SEM values of luciferase activity normalized for β-galactosidase activity or fold Gas5 expression compared to the baseline (Gas5 WT transfection in the absence of dexamethasone). *, $p<0.01$; n.s., not significant, compared to the condition tranefected with control plasmid and in the presence of dexamethasone (n=3). **(F)** Disruption of the Gas5 GRE-mimic prevents Gas5 from inhibiting the association of GR with *cIAP2* GREs and suppressing GR-mediated *cIAP2* transcription. HeLa cells were transfected with Gas5 WT- or GRE-1 Mut-expressing plasmid, treated with 10^{-6} M of dexamethasone. The abundance of *cIAP2* mRNA and exogenously expressed Gas5s, as well as the association of GR to *cIAP2* GREs in ChIP assays were evaluated with SYBR Green real-time PCR (right 3 panels) or regular PCR with adjusted PCR cycles (left panel). Similar abundance of GR was demonstrated by Western blotting. Bars represent the mean +/− SEM values of fold change in mRNA expression of *cIAP2* and exogenously expressed Gas5 molecules and fold change in the association of GR to *cIAP2* GREs. *, $p < 0.01$; n.s., not significant, compared to the baseline (in the absence of Gas5 transfection and dexamethasone treatment) (n=3).

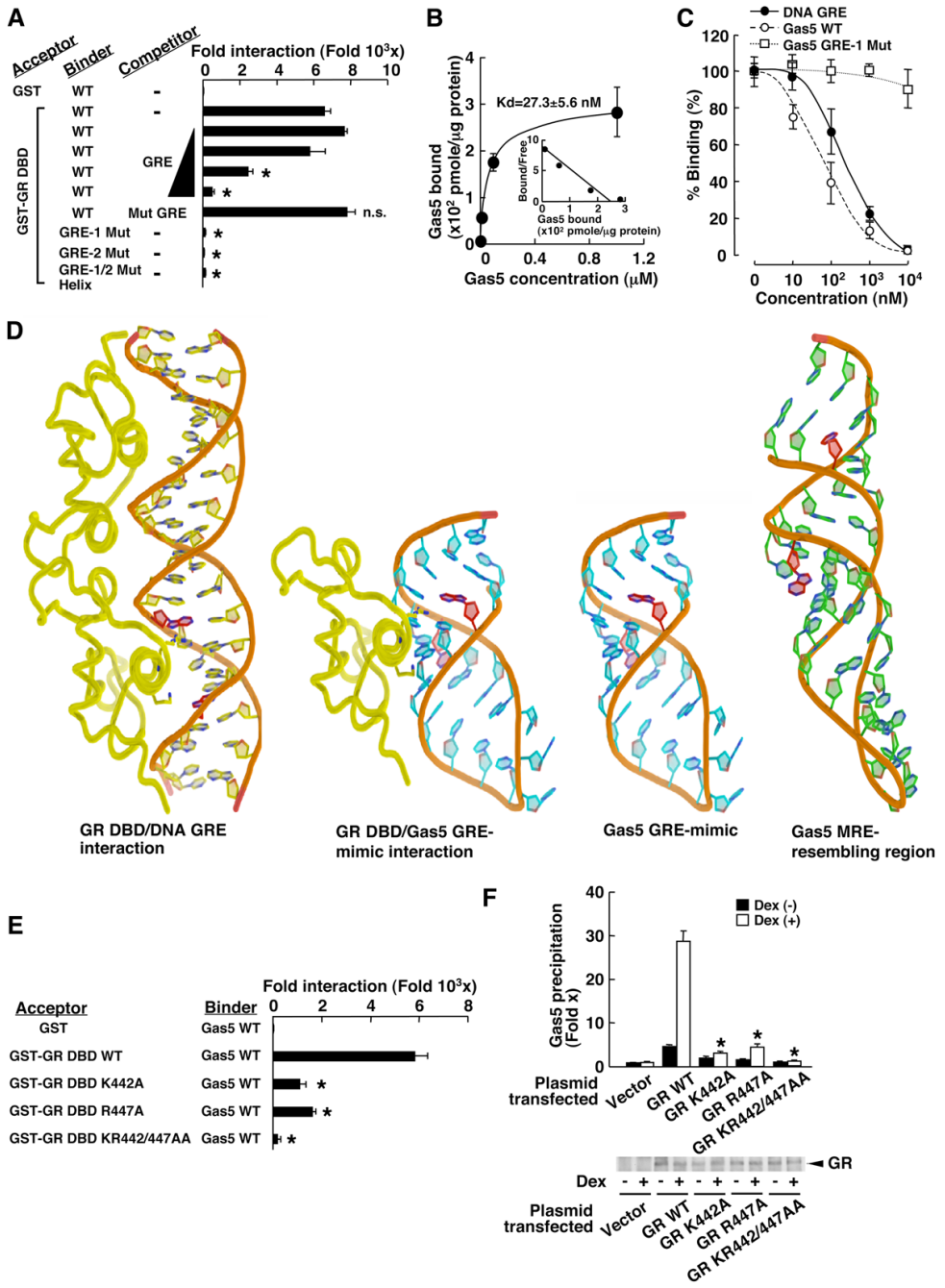

Fig. 9. Gas5 binds GR DBD through its double-stranded RNA GRE-mimic located at hairpin #5 and competes with DNA GREs for binding to GR DBD in vitro

(**A, B**) Gas5 directly binds GR DBD through its double-stranded RNA GRE-mimic in an in vitro binding assay. 10^{-4} M of indicated Gas5 RNAs was incubated with 1 μg of GST or GST-fused GR DBD bound to GST beads in the presence or absence of increasing concentrations (0, 10^{-5}, 10^{-4}, 10^{-3}, and 10^{-2}) of the double-stranded DNA GREs. Associated RNA was measured with the SYBR Green real-time PCR. Bars and circles represent the mean +/− SEM values of fold change in Gas5 association compared to the baseline (GST) and of the Gas5 molecules associated with GR DBD, respectively. (**B)** is a Scatchard plot (n=3). **(C)** Gas5 competes with FAM-labeled DNA GREs for binding to the GR DBD through its RNA GRE-

mimic in vitro. Oneμg of GST-fused GR DBD bound to the GST beads was incubated with 10^{-7} M of FAM-labeled double-stranded GREs in the presence of the double-stranded GREs, wild type (WT) Gas5 or Gas5 GRE-1 Mut RNAs. Symbols represent the mean +/− SEM values of % binding obtained by dividing the FAM-oriented fluorescence intensity of each point with those of the baseline (in the absence of competitors) (n=3). **(D)** Three-dimenstional structure of Gas5 GRE-mimic and its interaction model with GR DBD (left structure). Three-dimentional model of (left structure) GR DBD/DNA GRE association, (middle 2 structures) Gas5 GRE-mimic without and with GR DBD, and (right structure) Gas5 MRE-resembling region. K442 and R447 of GR DBD contact the G7 of the 5′ strand and the G4 of the 3′ strand (shown in red), which lie across from each other in the major groove of the DNA GRE (left structure) (36). The analogous base pairs in the Gas5 GRE-mimic (G540 and C554, respectively, shown in red) are calculated to be oriented similarly to those in the native DNA, possibly enabling them to form the hydrogen bonds with K442 and R447 of the GR DBD, respectively. The analogous base pairs in the Gas5 RNA MRE-resembling region (U453 and G474, shown in red) are calculated to be poorly oriented for potential binding to GR DBD. (**F:** Replacement of K442, R447, or both of GR DBD attenuates interaction of GST-GR DBD to Gas5 in vitro. 10^{-4} M of wild type (WT) Gas5 RNA was incubated with 1 μg of GST or the indicated GST-fused GR DBDs bound to GST beads. Associated Gas5 RNA was measured with SYBR Green real-time PCR. Bars represent the mean +/− SEM values of fold change in the association of Gas5 RNA normalized to baseline (with GST). *, $p<0.01$, compared to GR DBD WT (n=3). **(F)** Mutant GRs defective in either K442, R447, or both fail to bind Gas5. GR-deficient HCT116 cells were transfected with the control plasmid (Vector), pRShGRα (GR WT), pRShGRαK442A, R447A, or KR442/447AA and treated with 10^{-6} M of dexamethasone. Gas5 was coprecipitated with GRs with a GR LBD-specific antibody and GR-associated Gas5 was detected with SYBR Green real-time PCR. GR protein abundance was shown by Western blotting. Bars represent the mean +/− SEM values of fold Gas5 precipitation over the baseline (“Vector” in the absence of dexamethasone). *: $p<0.01$, compared to cells expressing GR WT and treated with dexamethasone (n=3).

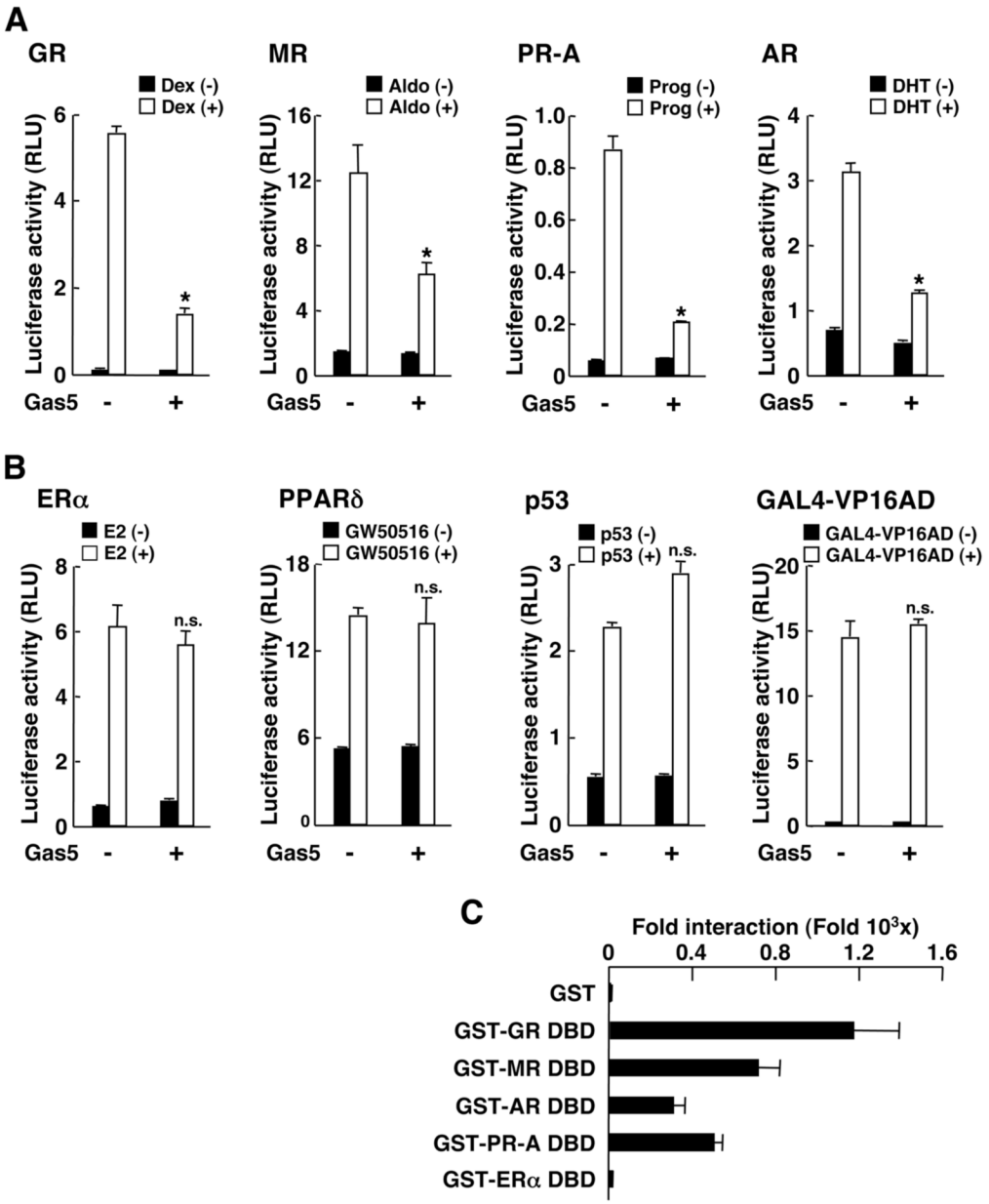

Fig. 10. Gas5 suppresses the transcriptional activity of several steroid receptors

(A) Gas5 suppresses mineralocorticoid (MR), progesterone-A (PR-A) and androgen (AR) receptor-induced transcriptional activity. (**B)** Gas5 does not influence ERα-, PPARδ-, p53- or GAL4-VP16-mediated transcription. For **A** and **B**, HCT116 cells were transfected with GR-, MR-, PR-A-, AR-, ERα-, PPARδ/RXRα-, p53-, or the VP16 activation domain (AD) fused to GAL4 DBD-expressing plasmid (GAL4-VP16AD), together with their responsive luciferase-expressing reporter plasmid and pSV40-β-Gal. Bars represent the mean +/− SEM values of luciferase activity normalized for β-galactosidase activity in the absence or presence of 10^{-6} M of dexamethasone (Dex) or progesterone (Prog), 10^{-8} M of aldosterone (Aldo), dehydrotestosterone (DHT) or estradiol (E2), 10^{-6} M of GW501516 (PPARδ agonist), or the indicated trans-acting factors. *: $p<0.01$, n.s.: not significant, compared to the baseline (in the absence of Gas5 transfection treated or transfected with indicated ligand or a *trans*-acting factor) (n=3). **(C)** Gas5 physically interacts with the DBD of the AR and PR-A, in addition to

that of the GR, whereas it does not bind the ERα DBD. 10^{-4} M of wild type (WT) Gas5 RNA was incubated with 1 μg of GST or GST-fused DBDs of GR, MR, AR, PR-A or ERα bound to GST beads. Associated Gas5 RNA was measured with SYBR Green real-time PCR. Bars represent the mean +/− SEM values of fold association of Gas5 RNA normalized for the baseline (with GST) (n=3).

Table 1

Primer pairs used in the SYBR Green real-time PCR for RNA quantification.

Gene name		Primer sequence
ADRP	Forward	5′-CTGTGGCCAGCACGATCAC-3′
	Reverse	5′-CTCACGAGCTGCATCATC-3′
cIAP2	Forward	5′-TCTAGTGTTCTAGTTAATCC-3′
	Reverse	5′-ACCACTTGGCATGTTGAACC-3′
Gas5	Forward	5′-AGCTGGAAGTTGAAATGG-3′
	Reverse	5′-CAAGCCGACTCTCCATACC-3′
G6Pase	Forward	5′-TCATCTTGGTGTCCGTGATCG-3′
	Reverse	5′-TTTATCAGGGGCACGGAAGTG-3′
GILZ	Forward	5′-GATGTGGTTTCCGTTAAGC-3′
	Reverse	5′-GATGTGGTTTCCGTTAAGC-3′
Luciferase	Forward	5′-CTCAACAGTATGAACATTTCG-3′
	Reverse	5′-CTGAAATCCCTGGTAATCC-3′
PEPCK	Forward	5′-GAAAAAACCTGGGGCACAT-3′
	Reverse	5′-TTGCTTCAAGGCAAGGATCTCT-3′
RPLP0	Forward	5′-GACATGCTGCTGGCCAATAAG-3′
	Reverse	5′-CAACATGTTCAGCAGTGTG-3′
SGK1	Forward	5′-CTATGCTGCTGAAATAGC-3′
	Reverse	5′-GTCCGAAGTCAGTAAGG-3′
U75	Forward	5′-CCTGTGATGCTTTAAGAG-3′
	Reverse	5′-CCTCAGAATAGAATTTCAG-3′

ADRP: adipose differentiation-related protein, cIAP2: cellular inhibitor of apoptosis 2, Gas5: growth arrest-specific 5, G6Pase: glucose 6 phosphatase, GILZ: glucocorticoid-induced leucine zipper, PEPCK: phosphoenolpyruvate carboxykinase, RPLP0: acidic ribosomal phosphoprotein P0, SGK1: serum/glucocorticoid-regulated kinase 1

Table 2

Primer pairs used in ChIP assays.

Gene name		Primer sequence	Band Size	Reference
ADRP	Forward	5′-CCTTAAGTGAGGAAATGAC-3′	121 bps	(31)
	Reverse	5′-CATCCCTGCTCTAATGAC-3′		
cIAP2	Forward	5′-GAGAATGGCACTGCAACTCAG-3′	345 bps	(25)
	Reverse	5′-CTACTATAGCTGCAGAAGTCC-3′		
G6Pase	Forward	5′-CAGACCCTTGCACTGCCAAGAAGCATG-3′	219 bps	(30)
	Reverse	5′-TATCCAGTATTCAGGTCAACCCAGCCC-3′		
GILZ	Forward	5′-CCTTAACTTCATCCAAACTG-3′	133 bps	(27)
	Reverse	5′-CACCAGAAGGAGCAAGAG-3′		
PEPCK	Forward	5′-GTTTCACGTCTCAGAGCTGA-3′	219 bps	(29)
	Reverse	5′-ACCGTGACTGTTGCTGATGC-3′		
SGK1	Forward	5′-TACCTCCTCACGTGTTC-3′	139 bps	(28)
	Reverse	5′-GTCGTCTCTGCACTAAAGG-3′		

ADRP: adipose differentiation-related protein, cIAP2: cellular inhibitor of apoptosis 2, G6Pase: glucose 6 phosphatase, GILZ: glucocorticoid-induced leucine zipper, PEPCK: phosphoenolpyruvate carboxykinase, SGK1: serum/glucocorticoid-regulated kinase